Innocent Bystanders: Carbon Stars from the Sloan Digital Sky Survey

Paul Green[1]

ABSTRACT

Among stars showing carbon molecular bands (C stars), the main sequence dwarfs, likely in post-mass transfer binaries, are numerically dominant in the Galaxy. Via spectroscopic selection from the Sloan Digital Sky Survey, we retrieve 1220 C stars, ∼5 times more than previously known, including a wider variety than past techniques such as color or grism selection have netted, and additionally yielding 167 DQ white dwarfs. Of the C stars with proper motion measurements, we identify 69% as clearly dwarfs (dCs), while ∼7% are giants. The dCs likely span absolute magnitudes M_i from ∼6.5 to 10.5. "G-type" dC stars with weak CN and relatively blue colors are probably the most massive dCs still cool enough to show C_2 bands. We report Balmer emission in 22 dCs, none of which are G-types. We find 8 new DA/dC stars in composite spectrum binaries, quadrupling the total sample of these "smoking guns" for AGB binary mass transfer. Eleven very red C stars with strong red CN bands appear to be "N"-type AGB stars at large Galactocentric distances, one likely a new discovery in the dIrr galaxy Leo A. Two such stars within $30'$ of each other may trace a previously unidentified dwarf galaxy or tidal stream at ∼40 kpc. We explore the multiwavelength properties of the sample and report the first X-ray detection of a dC star, which shows strong Balmer emission. Our own spectroscopic survey additionally provides the dC surface density from a complete sample of dwarfs limited by magnitude, color, and proper-motion.

Subject headings: astrometry – stars: carbon – stars: statistics – surveys

1. The Carbon Star Menagerie

Carbon (C) stars are defined loosely as those showing molecular absorption bands of carbon - C_2, CN or CH in their optical spectra (Secchi 1869). The key difference between C and M-type stars is their relative photospheric abundance of carbon and oxygen. In M stars, carbon in the stellar atmosphere is largely consumed by CO, but there's plenty of oxygen left for molecular species like TiO, which dominate M star spectra. C stars, by contrast, have such high C/O ratios that CO binds all the oxygen, with plenty of carbon remaining to form C_2, CN or CH molecular bands.

[1]Harvard-Smithsonian Center for Astrophysics, Cambridge, MA 02138

As far as we know, nearly all carbon in stellar atmospheres is produced by the triple-α process of helium fusion ($3\,^4\mathrm{He} \rightarrow\,^{12}\mathrm{C}$) in the interiors of red giant stars. C-rich material can only be dredged to the surface by episodes of strong convection associated with shell He-burning episodes (the so-called third dredge-up) that take place in asymptotic giant branch (AGB) stars. However, quite a variety of carbon-rich giant stars has emerged. C star classifications are well-described in Gray & Corbally (2009). Carbon giants are quickly identifiable by their strong bandheads, and easily detected to large Galactocentric distances, so offer excellent dynamical probes of the Galactic dark matter potential (e.g., Mould et al. 1985; Bothun et al. 1991).

Bright ($R \lesssim 13$) C stars were first classified in the Henry Draper Catalog as N (red) and R (blue) type. The N-type C stars are classic AGB stars - they are luminous ($\overline{M_K} \sim -7$) and massive $2 \lesssim M_\odot \lesssim 3$), with thin disk kinematics (Wallerstein & Knapp 1998; Lloyd Evans 2010). Many are strongly variable, with evidence for circumstellar dust. Based on their properties (abundances, photometry, kinematics, variability and luminosity), most stars previously classified as late R-type stars are probably misclassified N-type AGB carbon stars (Zamora et al. 2009). Many early R stars have been incorrectly classified as well, and in reality are classical CH stars (see below) or normal K giants. *Bona fide* early R stars have $\overline{M_K} \sim -2$, which puts them near the "red clump" of helium core-burning red giants. They show near solar metallicity, enhanced nitrogen, low $^{12}\mathrm{C}/^{13}\mathrm{C}$ ratios, no *s*-element enhancements, and normal binarity (McClure 1997), so the origin of their atmospheric carbon remains mysterious.

Less luminous C-rich giants with lower masses ($\lesssim 2M_\odot$) include the CH and Ba stars. Both types show strong carbon and *s*-process abundance enhancements, and neither type is found at AGB luminosities. CH stars have high space velocities and halo kinematics, and are metal poor with [Fe/H] values ranging from -0.5 to -1.7 (e.g., Vanture 1992, Wallerstein & Knapp 1998, and references therein). Barium II (Ba) stars are generally earlier F-, G-, and K-type objects, with young to old disk kinematics (Lu 1991). Both CH and Ba giants show evidence for a high binary frequency from radial velocity variations (McClure & Woodsworth 1990), with companions of about $0.6\,M_\odot$, which are presumably white dwarfs. There is also sparse UV photometric evidence for white dwarf (WD) companions to Ba giants (Böhm-Vitense et al. 2000). Ba dwarfs have significant far-UV excess compared to a control sample of normal F-type dwarfs Gray et al. (2011).

The mounting evidence for white dwarf companions to CH and Ba stars, and the theoretical expectation that carbon and *s*-process elements are dredged up and expelled only by "intrinsic" carbon producers (AGB stars), has led to the hypothesis that the enhanced abundances in CH and Ba stars are "extrinsic", i.e., attributable to previous episodes of mass transfer to the current primary from an AGB star, which has since evolved into a white dwarf. McClure (1997) studied a sample of 10 subgiant CH stars, and concluded that they were all post mass transfer binaries, with $900 < P < 4000$d. Given their binary orbital properties, both CH and Ba stars (Izzard et al. 2010) are thought to have suffered wind-accretion from a former AGB companion. Other extrinsic systems include the carbon-enhanced, s-process-rich, very metal-poor (CEMP-s) stars, with periods P from 200 - 2800d and amplitudes $K < 10$ km s^{-1} (but one with P=3.4d and $K = 52$ km s^{-1} (Lucatello et al. 2005). Carbon-enhanced metal-poor (CEMP) stars have an overabundance of carbon with respect to iron ([C/Fe]$> +1.0$), and represent a sizeable fraction of very metal-poor stars ([Fe/H]< -2.0). Radial velocity studies reveal that those that are *s*-process-rich (CEMP-s stars) are the

metal-poor analogs of classical CH stars (Lucatello et al. 2005; Izzard et al. 2009).

The discovery of the first *main sequence* carbon (dC) star G77-61 by Dahn et al. (1977) was at the time quite surprising, but it made clear that extrinsic processes can produce enhanced atmospheric abundances. The prototype dC G77-61 is a single-line spectroscopic binary showing no emission lines, and the companion, invisible in the optical range, is a WD with $T_{eff} <$ 6000 K (Dearborn et al. 1986). The hypothesis was that in a mass transfer binary (MTB), carbon rich material may be lost in a stellar wind from a thermally-pulsing AGB star and accreted by its companion main-sequence star. In the current epoch, the "polluted" companion, as an innocent bystander, could be either dwarf or giant, but the AGB donor has evolved to a white dwarf. This MTB scenario was strongly supported by the discovery additional dC stars recognized by their large proper motions during a search for faint high latitude carbon (FHLC) stars (Green et al. 1991).

Dwarf carbon stars are uniquely valuable systems, because even without any of the above signatures of binarity, they are all easily identifiable as post-MTB systems simply by their C_2 and CN bands. Furthermore, the properties of dCs may help us understand much about the amount of abundance-enhanced mass transferred, and how mixing occurs in the recipient dC. Depending on the host system properties, a current dC star may have inherited a significant portion of its mass (a third or more) by accretion, changing its overall structure in the process.

We have very little idea how common dCs really are. What are their space densities locally? Are they predominantly disk, thick disk, or spheroid? The relatively high temperature of the white dwarfs in known DA/dCs suggest an origin in the Galactic disk. Cooler DAs are likely much more prevalent, but simply harder to detect in the presence of a main sequence dC. In more metal-poor populations, less C-enhanced mass transfer is required to create C/O>1 atmospheres. G77-61 is itself one of the lowest metallicity stars known at [Fe/H]=-4 (Plez & Cohen 2005), so it could either be part of the elusive Population III stars formed very early in the galaxy, or perhaps more likely, its abundances have been affected by some process during its companion's binary evolution that selectively removed metals from the system (e.g., Waelkens et al. 1991).

Red dwarfs and red subdwarfs are low-mass main sequence stars. Because these stars are numerically dominant in the Galaxy, and have lifetimes exceeding a Hubble time (Laughlin, Bodenheimer & Adams 1997), they provide superb tracers of the chemical and dynamical evolution of the Galaxy. Only those examples that are carbon rich are easily identified from low/intermediate resolution optical spectra as post-mass-transfer binaries, and their present-day properties can provide a wealth of information about the history of their former AGB companions and the binary systems that they inhabit. This makes dCs an important class of object for study.

A large sample of FHLC stars with high quality multiwavelength data clearly provides a myriad of research opportunities. Carbon stars are now known to span absolute magnitudes from late-type dwarfs ($M_V \sim$ 10) to supergiants ($M_V \sim -4$). Luminosity discriminants from photometric colors and/or low/intermediate-resolution spectroscopy, as yet elusive, would be extremely valuable (Green & Margon 1994; Downes et al. 2004). Carbon giants can be used as dynamical tracers of the Galactic potential (e.g., Mould et al. 1985; Bothun et al. 1991) or signals of dwarf galaxies or their remnant tidal streams. Dwarf carbon stars, expected to be in binary systems, should be all radial velocity variable, yet the binarity and orbital parameters for dCs

as a population are completely unknown. A large sample of bright dCs should provide useful candidates for radial velocity monitoring. The frequency of different mass transfer scenarios for dCs, e.g., wind or Roche lobe overflow, can be modeled and probed. A reasonable sample of composite dC/WD systems can constrain the age since mass transfer for those systems. The space density of dCs can constrain the properties of ancient binary systems - their mass ratios, separations, and evolution (de Kool & Green 1995). Parallaxes can be obtained for some dCs, yielding more robust information on the distribution of their absolute magnitudes (Harris et al. 1998). Some of the brighter systems may soon be candidates for detailed modeling and abundance analysis (Plez & Cohen 2005), yielding information about the production of elements in extinct generations of AGB stars, dating back to the early Universe.

2. SDSS Sample Selection

In this paper, we use the Sloan Digital Sky Survey (SDSS; York et al. 2000) to greatly expand the sample of confirmed FHLC stars. Our goal is to select a large sample of C stars from the SDSS with minimal pre-selection by color, so that a wider variety of C stars can be studied than in the past. Using the SDSS DR7 database, after some experimentation, we chose to search for stars with spectra showing strong cross-correlation coefficients with the SDSS carbon star templates numbered 18 and 19, used for spectral cross-correlation by the SDSS project.[1] SDSS cross-correlation follows the technique of Tonry & Davis (1979), where the three highest cross-correlation function (CCF) peaks are found, fitted with parabolas, and output with their associated confidence limits. We required a best-fit peak CCF height of at least 0.3, which yielded about 400 stars, of which less than 0.5%, were not C stars. On the other hand, a minimum peak height of 0.1 yielded 8846 objects, few of which were C stars. After visual inspection of all spectra, we found that a minimum peak height of 0.15 yielded almost entirely C stars. The most common exceptions were quasars near $z = 3.66$ (where the blue wing of Lyα emission appears at the rest wavelength of the $\lambda 5636$ Swan band of C_2) and emission line or Seyfert galaxies near $z = 0.047$ (where the Hβ/[OIII] emission complex appears at the rest wavelength of the $\lambda 5165$ Swan band of C_2).

We recovered 1223 *bona fide* C stars in this procedure, which included 30 DQ stars. There are 1209 stars that are well-matched to template number 18, which has strong Swan bands. Of these, 422 also match with template 19, a redder template with strong red CN bands at $\lambda\lambda 7876, 7899$. Only 14 stars match with template 19 only, including 5 stars that show at best weak evidence for C_2 but which have strong red CN bands. In some cases, these stars are very red, so that while CN is evident, C_2 which may be intrinsically strong is lost in noise.

From SDSS DR8, we selected objects with spectroscopic class STAR and any subclass including 'Carbon', e.g., Carbon, Carbon_lines, or CarbonWD[2], as long as the velocity was within 3,000 km/sec of zero.

---

[1] See http://www.sdss.org/dr5/algorithms/spectemplates/. Template 20 yielded too many hot white dwarfs and/or blue stars.

[2] Although our primary interest is FHLC stars, we include CarbonWD because the classification may not always be correct.

The latter velocity criterion eliminates some QSOs incorrectly identified as carbon stars. Our selection initially yielded 1604 objects. 975 were in common with the DR7 velocity template selection, while 629 were newly-identified objects. However, after visual inspection, first we removed about 240 objects because of low S/N, and then another 40 were removed as having smooth blue continuum. (Some of these may well be DQ white dwarfs.) In the end, our list included 1264 spectra with visually-confirmed carbon molecular band features.

We merged the DR7 and DR8 lists and retrieved uniform DR8 data where available (13 DR7 objects had none), yielding 1510 spectra. There are multiple spectra for some objects, so that the number of distinct stars is 1390.

Generally, FHLC stars show a wide variety of colors, molecular and line absorption features, of which examples can be seen in Margon et al. (2002). Figure 1 shows a typical dC spectrum, for a high proper motion example newly reported here. The spectrum is overlaid with SDSS filter curves, which serves to illustrate the primary reason that C stars diverge from the stellar locus - strong C_2 molecular bands remove flux from the g bandpass. Our visual inspection of the spectra yielded just a handful of principal classifications: these include "normal" dC stars, 134 G-type FHLC stars,[3] 167 DQ White Dwarf Stars, and 9 composite spectrum DA/dC systems. Because they contain degenerate stars and are not the focus of the current work, we remove the latter two classes, leaving 1,211 objects in our main sample in Table 1. We discuss the principal classifications further below.

Comparing to the largest previous FHLC star compilation to date of 251 SDSS stars in Downes et al. (2004), our sample contains all but 24 of their objects. Most were rejected by our own visual inspection, because they had (1) very low S/N that made a C star classification doubtful, or (2) visual evidence in F- or G-type stars for strong G-band of CH, but not for C_2 or CN bands. For completeness, we list those objects in Table 2.

3. G-type FHLC Stars

One rather distinct group of C stars includes 134 objects with remarkably similar spectra, typically having blue continuua, strong C_2 bands, strong narrow Balmer and Ca absorption lines, but weak (usually non-existent) red CN bands. A typical example spectrum is shown in Figure 2. In the $(u-g)$ vs. $(g-r)$ diagram of Figure 3, these objects, shown with open blue circles, are strongly clumped. In the $(g-r)$ vs. $(r-i)$ diagram[4] of Figure 4, they hew close to the absolute mag locus of Kraus & Hillenbrand (2007), alongside the thin-disk sequence from about G2 - K0. For this reason, while Downes et al. (2004) referred to these as F/G carbon stars, we designate them simply as G-type FHLC stars. However, we note that the C_2 bands generally make FHLC stars appear bluer than similar-mass stars on the O-rich main sequence. The most likely absolute i-band magnitudes of G-type dC stars ($M_i \sim 7.25$; see § 10) puts them closer to K7 -

---

[3]The G-type FHLC stars are not intrinsically distinct or well-separated, so this number is a matter of definition - see § 3.

[4]Their colors are not so well distinguished in redder color-color diagrams.

M0.

4. DQ White Dwarf Stars

Another distinct class that we select are the DQ stars, which are white dwarfs showing atomic or molecular carbon features in their spectra. We find 167 such objects, listed in Table 3, which have the expected high proper motions and blue colors. The most commonly-accepted explanation for the DQs is dredge-up from the underlying carbon/oxygen core through the expanding He convection zone, which explains stronger C features at higher effective temperatures. DQs have been reviewed by Dufour et al. (2005), and some 65 SDSS examples have been studied (Koester & Knist 2006) spanning $5,000 < T_{\mathrm{eff}} < 10,000$ K, with some hot DQs now known to extend up to $\sim 24,000$ K (Dufour et al. 2008). Our DQ sample expands significantly on the existing list of recognized DQs, especially for objects with $(g-r) > 0.5$. DQs can appear redder in $(g-r)$ because they are cooler and/or lower [C/He] objects, but in our sample it is due in every case to extremely strong Swan bands of C_2 falling in the g bandpass. Several of these DQs show molecular absorption bands $\sim 100 - 300$Å shortward of the C_2 Swan bandheads. These "peculiar DQ bands" were discussed recently by Hall & Maxwell (2008) and Kowalski (2010). We do not discuss DQs extensively in this paper, because they are degenerates, so neither C giants nor dwarf stars, and are in any case thoroughly discussed elsewhere in the literature. However, the large number of DQs we find testifies to the sensitivity of our methods for detecting even weak or pressure-broadened carbon features, and for extending to objects that are significantly bluer than known C stars. A handful of DQs at low S/N have strange continuum shapes and/or evidence for CN molecular bands in the red, so may actually be composite DA/dC stars.

5. Emission Line Stars

Of our full sample of 1220 FHLC stars, 51 show clear Balmer emission lines upon visual inspection. Seven of those are DA/dC systems (§ 6). Of the remaining 44, 22 are definite dwarfs (see § 10), 20 are of unknown luminosity class, and 2 are giants (including Draco C-1, a known symbiotic star in the Draco dwarf galaxy). None of the 134 G-type stars show emission lines. The 22 emission line dCs represent 3% of the 724 definite dCs. The 2 emission line giants represent about the same fraction of giants, so emission lines do not at first glance appear to be a luminosity diagnostic, even in a probabilistic sense. Further studies of these emission line dCs are important, to determine the cause of the emission. Possibilities include coronal activity in the C star as a result of spin-up from accretion and/or tidal locking. Emission lines caused by irradiation by a hot companion only seems likely for the DA/dC systems.

6. Composite Spectrum DA/dC Stars

From our SDSS sample of C stars, a small but especially interesting subsample includes DA/dC composite spectrum systems. These show the usual clear C_2 bands, often along with red CN bands, but their

spectra display a strong blue continuum and the pressure-broadened hydrogen Balmer absorption lines typical of a DA white dwarf. There are only two such objects known to date (Heber et al. 1993; Liebert et al. 1994) [5], but objects like these are the 'smoking guns' that strongly support the post binary mass transfer scenario for the origin of dCs. We find 9 clear examples in our survey. Only one of these obvious composite systems, SDSS J151905.96+500702.9 is a known DA/dC system discussed by Liebert et al. (1994) as SBS 1517+5017 or CBS 311. Among our 8 newly-recognized DA/dC systems, all but two show Balmer emission lines in their SDSS spectra. At low S/N, it can be difficult to distinguish between a DQ and a composite DA/dC system. There are 3 such spectra in this category, but none show emission lines, and we believe they are likely to be *bona fide* DQ stars.

Because of the unique properties of DA/dC systems, there is widespread interest in them beyond the community of carbon star afficionados, including those involved in research of WDMS systems, close binaries, CVs, and planetary nebulae, etc. For this reason, we discuss the DA/dC composite systems in a companion paper (Green 2013).

7. Optical Colors

Spectroscopic fibers are assigned to SDSS photometric objects based on diverse criteria which evolved significantly over the course of the survey. Understanding the reasons why each object may have an SDSS spectrum is crucial to understanding the biases in any SDSS spectroscopic sample such as this one.

Of the 1220 FHLCs in our sample (including the 8 DA/dCs), the majority (56%) were targeted as QSOs. A quarter (24%) were targeted by the SEGUE project (objType=NONLEGACY), and just 17% were targeted as likely C stars using the color wedge from Margon et al. (2002) shown in Figure 4. The remaining 2.6% were targeted for a variety of other reasons, including white dwarf candidates, galaxies, reddening standards, and ROSAT counterparts (2).

Of the 134 G-type FHLCs, 97 (74%) were targeted by SEGUE based on optical colors, the bulk as low metallicity candidates. So the large fraction of G-type stars in our sample compared to Downes et al. (2004) is due to different targeting by SEGUE.

Our FHLC stars span a wide range of colors in the $(u-g)$ vs. $(g-r)$ color diagram of Figure 3. For a handful of stars, extreme colors are found resulting from saturation, or very faint u band mags with large errors. However, several important clusterings are in evidence.

DQ white dwarfs and composite DA+dC systems are well segregated using $(u-g) < 0.875\,(g-r)+0.5$ $\cup\,(u-g) <0.75$. Stars with blue $(u-g)$ but $(g-r)>0.6$ are either composite systems or DQ pec stars with extremely deep Swan bands dimming the g bandpass.

In Figure 3, we plot large red diamonds to show colors from the stellar SED compilation of Kraus & Hillenbrand

[5]We disagree with Downes et al. (2004) classification of SDSS J012747.73-100439.2 as a composite system.

(2007), which is most appropriate for O-rich main sequence thin-disk, solar-metallicity stars. Both C/O ratio and metallicity can strongly affect band strengths and therefore colors, explaining the shift of the FHLCs away from the main sequence disk locus of Covey et al. (2007), shown as a gray line. A clump of FHLC stars appears in a region offset just blueward of that, bordered by the following three lines shown by the blue dashed triangle $(u-g) < 2(g-r)+0.3 \cup (u-g) > 0.9 \cup (g-r) < 0.8$. But for a handful of exceptions, these $\sim$180 objects are all the G-type FHLC stars described in § 2. Based on a much smaller sample of these, (Downes et al. 2004) suggested that these G-type FHLC stars may form a continuum of properties with redder examples. Here, the G-type FHLCs seem strongly clumped, and appear to show a gap separating them from the general FHLC sequence (see also Figure 4). However, this is largely the effect of the SDSS fiber targeting algorithms. The deeper shaded region in Figure 4 shows the color wedge described in Margon et al. (2002) which was used to target potential FHLC stars for SDSS fibers. Since our sample is selected from SDSS spectra, FHLC stars within this color wedge are naturally over-represented relative to FHLCs elsewhere in the plane.

In the g vs $(g-r)$ color-magnitude diagram of Figure 5, most FHLC stars, at $(g-r) \sim 1.4$ and faint magnitudes, coincide with the locus of "thick-disk-like" ([Fe/H] $= -0.7$) stars seen at high Galactic latitudes ($|b| > 30\,$deg) in the SDSS (de Jong et al. 2010). The brighter G-type FHLCs near $(g-r) \sim 0.6$ instead coincide with the main-sequence turn-off stars of older, thick-disk or 'inner-halo-like" stars of intermediate metallicity ([Fe/H]$= -1.3$). The carbon molecular bands make FHLC stars bluer in $(g-r)$ making identification with these populations provisional at best. However, CH giants, which by their binarity are known to also be extrinsic, post-MTB systems, are also metal poor with [Fe/H] values ranging from -0.5 to -1.7 (e.g., Vanture 1992, Wallerstein & Knapp 1998, and references therein).

We assume that all dCs are in post-mass transfer binaries. Thus, they are clearly in systems where the initial primary has already turned off the main sequence, and indeed completed the AGB phase. If the mass ratio q of binary systems peaks near unity (Reggiani & Meyer 2011), then most dCs should be close to the turnoff mass, especially if the mass accretion is enhanced in higher mass bystanders. However, above a certain mass and effective temperature, the formation of C_2 molecules is suppressed, and at some point the C_2 features by which our FHLCs are identified diminish below detectability. Higher mass objects might still be identified as carbon-enhanced metal poor stars, but only with spectroscopy of significantly higher resolution and S/N.

We thus hypothesize that the current-day main sequence primaries in post-AGB MTB systems should mostly be near the turnoff. Because they are more massive and brighter, among post-MTB survivors, such stars should be preponderant in a magnitude-limited sample such as the SDSS. At higher masses, they may also be more effective at accreting abundance-enhanced material. Since they are essentially innocent bystanders to mass accretion, one might expect a smooth trend in color and mass for these stars in Figure 4. Instead, there is a distinct clump of G-type FHLC stars, separated by a gap from redder dCs. This is probably caused by two effects. First, the SDSS color selection wedge for C star spectroscopic candidates causes the cutoff of dCs near $(g-r)= 0.9$. If not for that color selection wedge, we would expect a smooth trend of FHLC stars across the gap that spans $0.8 < (g-r) < 0.9$. Second, as the G-type FHLCs become progressively hotter and bluer, the carbon molecular bandheads weaken (see Figure 6), until they are no

longer detectable for stars bluer than about $(g-r)$ =0.4. Several effects thus conspire to make the G-type FHLC stars stand out in a clump in our sample. Significant fractions of bluer stars may well have mass transfer-enhanced abundances at masses higher than this, but more detailed analysis of their spectra are required, probably at higher resolution and S/N.

The red end of the FHLC sequence is also not inconsistent with the MTB scenario; dC stars taper off at colors equivalent to mid-M dwarfs. This is also where the SDSS magnitude limits probe too low a volume to have significant surface density of later types (see e.g., Figure 8).

8. Multi-wavelength Data

Since many of our C stars have significant proper motions, we have to be somewhat liberal in the positional search radii used for matching to multiwavelength catalogs from imaging obtained at a variety of epochs. Unless otherwise specified, we retrieved and matched catalogs from the Virtual Observatory (VO) using the TOPCAT tool.

We matched all objects in our SDSS C star catalog to the 2MASS All Sky catalog using a $3''$ search radius. 99% of matches found were within $2''$. We also matched the C star catalog to the UKIDSS DR6 to within r =$2''$, but found no matches at $r > 1.5''$.

The Galaxy Evolution Explorer (GALEX) all-sky UV survey (Martin et al. 2005) makes it feasible to detect hot white dwarfs in unresolved binaries with main sequence companions as early as G-type and K-type, and cooler WD with companions early M-type or later. We matched to GALEX GR6 UV catalog using a $4''$ search radius, but found no matches beyond $2''$. Our shift and rematch experiments yield a ∼3% spurious match rate. GALEX GR6 covers most of the SDSS footprint.

To search for mid-infrared (3.4, 4.6, 12, and $22\mu m$) photometry, we uploaded our object catalog to IRSA[6] for matching to the Preliminary Release Source Catalog from NASA's Wide-field Infrared Survey Explorer (WISE; Wright et al. 2010) using a $4''$ search radius. 90% of matched WISE sources have total WISE astrometric uncertainty $< 1.1''$ ($0.8''$ per coordinate). Actual SDSS/WISE match separations cutoff sharply at about $2''$, with a tail (encompassing some 14% of objects) out to $4''$.

8.1. GALEX Ultraviolet-Detected Stars

GALEX photometry is in two bands, far- and near-ultraviolet (F and N) with $\lambda_{\mathrm{eff}} = 1516$Å and 2267Å, respectively. Strong UV flux such as might be detected by GALEX in stellar systems can arise from a very hot blackbody, such as a hot white dwarf, or may also be associated with stellar activity (Pagano 2009). In our full sample of 1390 SDSS stars showing carbon (including DQ WDs), we find 318 GALEX detections.

---

[6]http://irsa.ipac.caltech.edu/cgi-bin/Gator/nph-dd

We may expect that FHLCs with GALEX detections should arise primarily from systems with hot white dwarf companions. As evidence for our capacity to detect such systems in GALEX GR6, 136 of the 318 GALEX detections are DQ white dwarfs, which is 80% of the (167) DQs in our sample. Excluding the DQs leaves 182 of 1220 FHLCs detected by GALEX, or 15%. This is about 5 times the (3%) spurious match rate, so the majority are truly associated detections.

Of these 182 GALEX-detected FHLCs, 90 are G types. These 90 represent 68% of all the (134) G-type FHLCs in our sample, an extremely high detection fraction. In comparison, the fraction for "typical" FHLC stars (neither G-type nor composite) is only 8%. However, G stars are both brighter and bluer than typical FHLC stars. Figure 7 shows the (NUV-r) vs ($g-r$) colors of our FHLC sample. Limiting both G and typical samples to be brighter than the 75th percentile of $r = 18.27$, the detection fractions are 76% and 21%, respectively. Limiting instead both samples to be bluer than the 75th percentile of ($g-r$)=0.666, the detection fractions are 70% and 45%, respectively. We therefore conclude the G-type FHLC stars indeed have stronger NUV fluxes than other FHLC stars, independent of their optical colors.

However, when we match the predominantly normal (high proper motion) stars in the Gould & Kollmeier (2004) catalog to GALEX, we find that stars with G-type colors ($g-r$)< 0.8 have a 72% GALEX detection rate, compared to a 6.5% rate for redder stars. In other words, a GALEX NUV detection pulls out the bluer brighter stars (most likely the metal-poor turnoff stars) at a rate approximately independent of carbon enhancement. So, we conclude that the high NUV detection rate of G-type FHLC stars is not evidence for hot white dwarf companions.

Only 3 of the 90 NUV-detected G-type FHLCs have FUV detections, which could signal hot WD companions. Besides having a hot white dwarf component, UV brightness can arise in young, active objects, from their active regions, transition regions, or chromospheric emission. However, none of the G-type FHLC stars show emission lines.

After excluding the G-types, of the remaining GALEX-detected FHLCs, 10 indeed have strong emission lines. One of those is Draco C-1, a known symbiotic star in the Draco dwarf galaxy. Of the 9 galactic GALEX-detected objects with emission lines, 6 are clearly DA/dC composites, showing evident broad Balmer absorption in the blue.

Indeed, of all 17 non-G-type galactic objects detected in the FUV band, 7 are composite DA/dC systems. It is of interest to determine what sorts of non-G-type, non composite FHLC stars are FUV-detected. Of 9 such systems two are clearly giants, with $r < 16$ and undetected proper motion. SDSS J 063313.18+840900.1 and 144945.37+012656.1 probably have hot white dwarf companions that are overwhelmed in the optical by the luminous cool giant. At least one or two others may be G-type or composites misclassified due to low S/N spectra. We venture that the rest, especially those with insignificant proper motions may be subgiants harboring hot white dwarfs, or possibly spurious matches near QSOs.

Red giants are cool, so should not have significant UV emission unless a WD companion is accreting material thrown off by the RG wind, i.e., a symbiotic star. In such a case, very soft X-ray emission may be detected as well, and strong emission lines should be present. As an example, Draco C-1 is detected by both ROSAT and GALEX and has strong high ionization optical emission lines; § 14.2.

We consider that cool (non G-type, i.e., $(g-r) > 0.8$) FUV-detected FHLC stars without detectable proper motions or strong emission lines are quite likely to be dC systems.

8.2. Near Infrared Properties

We match the sample to the 2MASS point source catalog. Joyce (1998) explained the unusual location of dC stars in the JHK color-color diagram, via collision-induced absorption, which is predicted to suppress molecular absorption features in the near-infrared for stars of low metallicity and high surface gravity. Downes et al. (2004) noted that a large fraction of objects satisfying a more restricted color range of $(J-H) < 1.2$ and $(H-K) > 0.29167(J-H) + 0.25$ were dwarfs.

Figure 14 shows that within the magnitude range of our SDSS spectroscopic sample of FHLC stars, near-IR colors seem to distinguish a region $(H-K) > 0.3$ where the vast majority of stars are dwarfs (green crosses), with most giants (red dots) clustered at bluer values. Use of $(r-i)$ color for the ordinate axis creates an even stronger segregation of giants, at least within our sample. However, we see that in Figure 15 inclusion of a wider sample of known C giants further weakens the apparent strength of near-IR colors alone as a photometric luminosity discriminant.

However, cool N-type AGB C stars tend to populate the region $(J-K)_0 > 1.4$ and $(H-K)_0 > 0.45$, a selection used by Demers & Battinelli (2007) to select thin/thick disk velocity probes. We find 37 stars that satisfy these criteria.

8.3. WISE Mid-Infrared-Detected Stars

Since dCs are thought to have accreted mass dumped from an AGB star, there may be cases where a redsidual debris disk can be detected.

WISE surveyed the entire sky at 3.4, 4.6, 12 and 22 microns in 2010, achieving 5-σ point source sensitivities better than 0.08, 0.11, 1 and 6 mJy in the four bands (for unconfused regions on the ecliptic plane). The WISE All-Sky data release (March 14, 2012) includes 563,921,584 point-like and resolved objects with S/N> 5 in at least one band. Of the 1035 FHLCs matched to SDSS, we eliminate from our analyses the small fraction (2%) of sources that have any saturated pixels or are deblended (nb= 1), or have more than one PSF component in the profile fitting (nb> 1).

Figure 8 shows optical vs. WISE colors for FHLC stars. N-type AGB stars can be effectively separated in this plot by their extreme redness; most FHLC stars with $(i$–[4.6])> 4 have no proper motions, and are likely on the AGB. A similar plot using $(i-K)$ is equally effective. FHLC stars in these plots appear to be offset from the main sequence of high-p.m. dwarfs merely by their redder $(g-r)$ colors, caused by C_2 bands falling within the g filter bandpass (Figures 1 and 2).

9. Proper Motions

The proper motion catalog of Munn et al. (2004) combines astrometry from the USNO-B and SDSS imaging surveys. Our criteria for a significant proper motion are as follows: (1) at least one USNO-B detection and one SDSS detection per source (nfit > 2), (2) proper motion in at least one coordinate larger than 3σ, where σ is the proper motion uncertainty in that coordinate, and (3) total proper motion larger than $11 \, \mathrm{mas \, yr^{-1}}$.

Reduced proper motion (RPM) correlates well with absolute magnitude (Strömberg 1939). Where the absolute magnitude $M = m + 5 + 5 \log \pi$ (where π is the parallax in arcsec), RPM are calculated as $m + 5 \log \mu$ (where μ is the total proper motion in arcsec per year). If all stars had te same transverse velocity, only a zero-point shift would be needed to match a color-RPM to a color-magnitude locus. In an color-RPM diagram, subdwarfs should be offset from main sequence stars because they have large transverse velocities and because at the same color they are dimmer.

In Figure 11, we plot the reduced proper motion (RPM)

$$H_r = r + 5 \log \frac{\mu}{\mathrm{mas \, yr^{-1}}} - 10 - 1.47 \, |\sin b|$$

against $(g - i)$ color for stars with significant proper motions. The final term in H_r, dependent on Galactic latitude b, compensates for the vertical offset of the RPM distribution of samples of stars at different b (Salim & Gould 2003).

The dC stars (black dots), appear to fall below the red main sequence dwarfs (densest region on the right), closer to the subdwarfs (lower diagonal track to the left), indicating they may either be slower moving halo dwarfs, or perhaps thick disk stars. However, the apparent dCs' offset in H_r is likely *weakened* by the fact that dCs of a given mass or absolute magnitude appear redder than their O-rich main sequence counterparts because of the strong C_2 bands falling in the g passband. So we suggest that the true dC offset in absolute magnitude may indeed correspond to the subdwarf population. G-type stars (blue circles) simply represent earlier type, more massive subdwarfs.

10. Absolute Magnitudes

The absolute magnitudes of carbon dwarfs are poorly known. As part of the USNO parallax program, Harris et al. (1998) found that the 3 dCs they measured had very similar luminosities ($9.6 < M_V < 10.0$), $\sim 2 \, \mathrm{mag}$ subluminous compared to normal disk dwarfs of similar colors and solar-like metallicities. This could be due to low metallicity, enhanced He, and/or the strong molecular lines in the optical, but the kinematics are consistent with a spheroid population.

We find 7 dCs in our sample with additional ground-based parallax measurements provided by Hugh Harris (private communication). For these, we find mean absolute magnitudes $M_r = 9.0 \pm 1.1$, $M_i = 8.5 \pm 1.1$, and $M_K = 6.0 \pm 0.9$. The mean M_V is 9.4 ± 1.5. Within the small sample of these dCs with parallax measurements, there is no significant correlation between absolute mag and color, to encourage us to predict

dC luminosity based on color. However, this is at least in part because the dCs with parallax measurements span a relatively narrow color range of $0.4 < (r-i) < 0.6$, with mean 0.49 ± 0.07. If we exclude composite systems and G-types from our dC subsample (yielding 656 objects), the mean $(r-i)$ is similar: 0.45 ± 0.12. However, we certainly expect a range of absolute magnitudes for FHLC stars, and in particular the G-types extend to $(r-i) \sim 0.1$, and show smaller proper motions, and so are likely to be more luminous.

We examined a variety of color-color plots for the C stars, to see if we could determine a color that closely tracks the O-rich main sequence. It is clear from the C star spectra that molecular band features spanning a huge range of equivalent width routinely affect the g bandpass (spanning $\sim 4100 - 5400$Å). The r band ($\sim 5600 - 6800$Å) may also be affected, but less so, and the i band even less ($\sim 6900 - 8100$Å), except where strong CN bands may occur.

We had hoped that the near-IR colors would offer a smaller dispersion around the O-rich main sequence, but the 2MASS-matched sample shows wide scatter in all the near-IR colors. C star colors appear to hew closest to the O-rich main sequence locus in the $(r-i)$ vs. $(i-z)$ plot for the range $0.1 < (r-i) < 0.8$, which corresponds to their spectral types $\sim$G1 through M1 and includes 96% of the C stars. Since the locus of median colors in this color range closely follows $(i-z) = 0.6(r-i) - 0.04$, either color alone could be used just as well, so we choose $(r-i)$ colors (since errors are generally lower than for $(i-z)$). For each star in our sample, we can derive an estimate of the absolute i magnitude M_i, and using the main sequence absolute magnitudes from Kraus & Hillenbrand (2007), despite the fact that their sequence consists primarily of disk stars. Using this method, however, we find that the derived M_i values for dCs are ~ 1.75 mag brighter than those of the parallax-measured dCs in the same color range. For definite dCs, we therefore derive M_i values from the $(r-i)$-M_i relation of Kraus & Hillenbrand (2007), but adding an offset of 1.75 mag to estimate their true absolute magnitudes. This admittedly crude approximation can then be used to estimate a photometric parallax distance. Further support for our adopted method comes from the fact that transverse velocities then taper off strongly by about 400 km s^{-1} (rather than ~ 800 km s^{-1}) with only a handful above 600 km s^{-1} (Figure 13).

10.1. Definite Dwarfs or Giants

Given the sensitive proper motion detection limits, does a significant proper motion guarantee that the star is a dwarf? Given an observed proper motion, simply assuming that the star is gravitationally bound to the Galaxy sets an upper limit on its distance. The upper limit, combined with the observed magnitude, sets a lower limit to absolute magnitude.

Recent estimates from the RAVE survey (Smith et al. 2007) place the local Galactic escape velocity lies within the range $498 < v_{esc} < 608$km/s. We conservatively assume that the Galactic escape velocity $v_{esc} = 600$ km s^{-1}. Subgiant stars can be found at absolute i band magnitudes $M_i \lesssim 3$. We adopt that anything less luminous than $M_i = 3$ must a dwarf. Figure 12 shows that indeed virtually every object with detected proper motions is definitively a dwarf. A handful of possible exceptions that tiptoe beyond the subgiant boundary are G-type FHLC stars, which may be expected as they are near the main sequence turnoff. We

adopt that any FHLC star in our sample with a detected proper motion as defined in § 9 is a dC, and there are 729 examples, marked Class=d in Table 1, about 6 times as many as previously known (Downes et al. 2004), and 59.7% of our total FHLC sample.

Conversely, can we determine that an FHLC star is definitively a giant? We follow the line of argument established in Downes et al. (2004). First, we estimate our detection limit for proper motions, which we determine to be $\mu^{\min} \sim 15$ km s^{-1} because 90% of objects with significant proper motion exceed that value. Then, using the M_i estimates established above, we derive a photometric parallax distance for objects with a significant proper motion, and use that to calculate transverse velocity v_t. A cumulative histogram reveals that 90% of dCs have $v_t > 50$ km s^{-1}. Assuming that dCs have $v_{t,\min} = 50$ km s^{-1}, then a non-detection places a *lower* distance limit on an FHLC of

$$d_{\min} = v_{t,\min} \, (1000/4.74 \, \mu_{\min}) = 1055 \, \mathrm{pc}$$

where $v_{t,\min}$ is in km/s and $\mu_{\min}$ is the total proper motion in mas/yr. From $d_{\min}$, we find the least luminous absolute magnitude $M_{i,\max}$ that a $v_t \sim 50$ star must have to have escaped proper motion detection, and compare that to a dwarf/giant threshold criterion. Figure 13 shows that dCs quite likely achieve magnitudes as luminous as $M_i' \sim 6.3$, which we therefore adopt as our threshold. Any FHLC star with a measured but insignificant proper motion, but an i-band magnitude

$$i < M_i' - 5 + 5 \log(d_{\min}) = 16.4$$

we consider to be a definite giant, and are marked as such (Class=g) in Table 1. With this definition, we find 59 giants, or 4.5% of our full FHLC sample.

Objects with no proper motion measurements, or insignificant measured proper motions and $i > 16.4$, are marked as Unknown (Class=u). There are 419 objects in this class, or 34.3% of our sample.

If we restrict consideration to the 1050 objects with existing proper motion measurements, the fraction with dwarf, giant, or unknown luminosity class becomes 69.4%, 23.7%, and 6.9% respectively.

11. Velocities

SDSS tabulates radial velocities obtained two ways: from cross-correlation using SDSS commissioning spectral templates (Stoughton et al. 2002), and from comparing to the (resolution-degraded) ELODIE library spectra as described by Moultaka et al. (2004). While for typical stars, the ELODIE velocities are considered more reliable, the ELODIE library does not contain any carbon stars. Even for CEMP stars, which lack the striking C_2 and CN bandheads of our FHLC stars, Lee et al. (2008) noted that cross-correlation with special templates based on synthetic spectra are generally required to produce reliable radial velocities. Therefore, we judge a detailed study of the kinematical properties of the population to exceed the scope of this paper. We nevertheless show in Figure 9 the radial velocities of the sample plotted against derived transverse velocities v_t. Since v_t estimates require significant proper motions (§ 9), as well as distance estimates based on our estimates of absolute magnitude, as described in § sec:absmag, the plotted sample is

limited to the 621 FHLC stars fulfilling those criteria. The strong overlap of the redder dCs with the G-types, illustrate that they likely originate in a similar population. Figure 9 (right panel) shows a histogram of the estimated space velocities v_{sp} of the same sample. The median space velocity is 208 km/s, while the mean is 225 ± 133 km s^{-1} . The distribution of v_{sp} for the G-type dCs in this sample is not significantly different than the overall distribution.

12. "N"-type AGB stars

The classical "N"-type AGB C stars have very red colors and often show strong CN bands, in some cases with Balmer emission lines as well. Such stars' spectra are quite distinct in appearance from dCs, unlike the spectra of warmer R or CH giants. As such, faint examples may be useful tracers of the Milky Way gravitational potential at large Galactocentric distances.

We searched our sample for spectra noted as being "red" and/or with "strong CN", and removed objects with weak C_2 lines or (in just one case) a detectable proper motion. This left 14 stars, 2 of which are known in the dSph galaxy Leo II. One other star, SDSS J125149.87+013001.8, was recognized as an N star in Downes et al. (2004). The remaining 11 are all likely newly discovered high galactic latitude N stars.

The 17 Galactic N stars measured by Hipparcos have mean absolute magnitudes $M_V = -0.8 \pm 1.3$ and $M_K = -7.0 \pm 1.1$ (with similar median values; Wallerstein & Knapp 1998), which we take as -1 and -7 respectively, given how uncertain we are about the similarity of that sample to our own.

Using $M_K = -7$, the N stars in Leo II yield photometric distances of 235 kpc for SDSS J111312.83+221114.1 and 200 kpc for SDSS J111320.64+22 1116.3, consistent with published distances (van den Bergh 2000). The remaining N star candidates range from 30 to 160 kpc in (K-band estimated) distance.

We note that the two N star candidates SDSS J144448.86-011056.2 and SDSS J144631.08-005500.4 are within $30'$ of each other, and having similar magnitudes, colors, and velocities, may well signal the existence of a dwarf galaxy or tidal stream. Their K magnitude (~ 11) places them at a distance from us of about 40 kpc, with mean Galactic coordinates $l \sim 352$ deg, $b \sim 51$ deg. No overdensity in this region is previously noted in the catalog of neighboring galaxies of Karachentsev et al. (2004), but we suggest that deeper images and color-magnitude searches may reveal something in the vicinity.

We note that *every* star that met our N star candidate criteria has $(J-H) > 0.8$, as do all the bright N stars from Alksnis' (2001) catalog shown in Figure 15. None of our N star candidates has a GALEX detection. Therefore, we are confident that, while it may not be complete, our method is pure, i.e., it does produce a list of *bona fide* AGB N stars.

13. C Stars in Local Group Galaxies

We assembled a list of Local Group dwarf galaxies from the McConnachie (2012),[7] having distance moduli <24.5 mag. At these distances, the most luminous AGB C stars would have $V \lesssim 20.5$, and therefore could be bright enough for SDSS fiber spectroscopy[8]. We find 10 FHLC stars from our catalog that fall within a degree of their approximate central Local Group galaxy coordinates. Two of these have significant proper motions, and are likely to be foreground dC stars.

Of the remaining 8, 3 are known to be in Draco[9](Downes et al. 2004).

We also find 3 C stars already known in Leo II (Aaronson et al. 1983; Vogt et al. 1995). At the distance of Leo II ($\sim$205 kpc), they have $M_r \sim -2.8$. SDSS J111324.84+220916.8 has seemingly bizarre $(g-r)$ colors and a significant proper motion measurement, but both are due to blending with nearby objects in Draco.

One C star, SDSS J132755.56+333521.7 was recently noticed by Zucker et al. (2006) among SDSS spectra of stars in a newly discovered local group dwarf galaxy in Canes Venatici. It has $M_r \sim -2.5$, typical of a CH carbon giant.

The one remaining star SDSS J095955.57+304058.5 with $r = 20.61$ may well a member of Leo A. There is no proper motion measurement available for this object; a firm upper limit to its motion would strengthen the argument for membership. If this object is a luminous AGB star ($M_r \sim -3.6$) and, by comparison to the known Local Group C stars herein has $(r-K) \gtrsim 2$, then at the distance of Leo A ($\mu = 24.2$), the expected near-IR magnitude $K \sim 18.6$ is too faint for 2MASS, and indeed the object is not detected therein.

Leo A is a dwarf irregular (dIrr) galaxy. C stars are less common, but not unknown in dIrr galaxies. For instance the Magellanic dIrr DDO 190 (also known as UGC 9240) contains many (photometrically-identified) C stars, which is taken as evidence for the existence of an old stellar halo (Battinelli & Demers 2006). Spectroscopically-confirmed C stars in dIrr galaxies appear to be rare in the literature, so this object may seems likely to be a valuable addition.

14. X-rays from Carbon Stars

Since we now know that most C stars are in mass transfer binary systems, a fraction of them may still have hot WD companions. For close binaries, there may be accretion onto the WD, or even coronal activity in the C star as a result of spin-up from accretion and/or tidal locking.

We searched several X-ray catalogs for positional coincidence to our sample, using a somewhat gen-

---

[7]Also thanks to Richard Powell for compiling http://www.atlasoftheuniverse.com/galaxies.html.

[8]80% of our FHLC stars have $V \lesssim 20.5$.

[9]In fact, SDSS J171942.39+575837.7 has no proper motion measurement, but has $v_r = -278 \pm 3$, quite similar to the other known Draco C stars.

erous matching radius, permissible because both X-ray sources and carbon stars are rare on the sky. We searched the Chandra Source Catalog (version 1.1; Evans et al. 2010) with a $6''$ radius and found no matches. Our results from XMM-*Newton* and ROSAT catalog searches are described below.

14.1. SDSS J125017.9+252427.6

We searched the 2XMMi-DR3 (Watson et al. 2009) with a $6''$ radius and found a single match to SDSS J125017.9+252427.6. SDSS J125017.9+252427.6 is a bright ($r = 16.4$) dC star with spectacular bands of C_2 and CN, along with Balmer emission lines visible from Hα to Hϵ. It has a highly significant proper motion (34.4 ± 4 mas/yr). The positional separation from the XMM-*Newton* source is just $1.8''$, while the nearest $g < 22$ optical counterpart is at $35''$. Its optical and IR colors are not unusual for a dC, and it is not detected by GALEX. Assuming $M_r = 9$ for a dC puts this object at $\sim$300 pc. From the XMM reported flux (0.2-2 keV) of 6.36×10^{-15} erg cm^{-2} s^{-1}, we derive an X-ray luminosity $\log L_X = 6.9 \times 10^{28}$ erg s^{-1}. Such a luminosity is rather typical for X-ray detected stars in the Chandra serendipitous survey (CHESS; Covey et al. 2008).

14.2. ROSAT Detections

We also searched the ROSAT All-Sky Survey Faint Source Catalogue (RASS-FSC; Voges et al. 2000), using a $25''$ radius. This radius yields a spurious matching rate of about 35% for SDSS magnitude limits (Agüeros et al. 2009).

We rediscovered that the known C star in the Draco dwarf galaxy, Draco C-1 (Aaronson et al. 1982) is a ROSAT detection. Draco C-1 is also detected by GALEX, and as expected, shows no significant proper motion. Its SDSS spectrum features powerful Hα emission ($W_\lambda = 110 \pm 10$) with a broad base, and strong emission lines of He I and He II, as noted by Margon et al. (2002). Draco C-1 is a known symbiotic star (a red giant transferring mass to a WD companion), and variable in both flux (Kinemuchi et al. 2008) and radial velocity (Olszewski et al. 1995), the latter probably caused by orbital motion.

15. Completeness Studies

Our SDSS sample therefore represents a heterogeneous sample, but is not strongly biased toward the initial FHLC star selection color wedge. However, even within the SDSS color wedge (and certainly without) the fraction of objects that were sampled, and which turn out to be C stars is a complex function of competing SDSS fiber assignment priorities and their evolution. We therefore have undertaken our own experiment specifically to constrain the fraction of dC stars within the color wedge.

Using the 1.5m Tillinghast reflector and FAST spectrograph at the Fred L. Whipple observatory on Mt Hopkins, we obtained FLWO1.5m/FAST spectroscopy of dC candidates. To arrive at our FAST sample,

we chose from SDSS DR7 the color locus where >90% reside, which corresponds closely to the color plane $(g-r)> 1.587 (r-i) + 0.534$ examined by (Margon et al. 2002, see our Figure 4). We then require a minimum proper motion of 11 mas/yr from SDSS/USNOB, combined with reasonable quality criteria (e.g., p.m.$> 3\sigma$, $r >15$ to avoid saturation). Among the resulting 171,650 objects, there were 2334 with SDSS-II spectra. Inspection of these yielded 165 *bona fide* dCs, 43 more more than published at the time. However, all those were in a narrower wedge of color, allowing further restriction by $(r-i)> 0.3556(g-r)$ - 0.17 (Figure 4).

To construct a pilot spectroscopically complete sample, we selected a random subsample of 300 stars within this narrower color wedge, also having high quality photometry, total proper motion > 40mas/yr and observable efficiently with FAST: $15 < r < 17$ and $\delta > -05$. Our pilot sample is uniform, homogeneous, and randomized so that completeness is easily derived. From May 2009 until May 2010, we obtained 291 FAST spectra, spanning 3470 – 7400Å at 1.5Å/pixel resolution. We find 10 of these are *bona fide* new dC stars, listed in Table 4, which corresponds to a fraction (from the β function distribution) of $3.6\pm0.1\%$. Three of these objects also have SDSS spectra. Our sample of high quality dC spectra are rather typical, except for one object discussed below.

Our final photometric criteria are shown explicitly as CasJobs query language in Appendix A. The full sample of SDSS DR7 objects meeting these criteria constitutes 1,973 stars. Applying the dC fraction from our observed FAST sample implies that there are 71 ± 2 such bright, high proper motion dCs. The SDSS DR7 sky area with $\delta > -05$deg represents about 10,770 degsq, so that the surface density of such objects is about one per 150 deg^2. This number can be used to constrain the dC population model, and thereby the history of AGB stars and binary mass transfer in the Galaxy. Such modeling is well beyond the scope of the current work, since a full model of dC populations should include their likely distribution of absolute magnitude, color, space density, kinematics, and scale height (de Kool & Green 1995). Indeed, several distinct populations are likely needed, halo, thick and perhaps even thin disk.

As part of our FAST program we discovered the only known dC/dM spectroscopic binary star, which must also harbor a white dwarf. The spectrum of SDSS J184735.67+405944.2 in Figure 16 has clear (relatively weak) C_2 absorption, strong Balmer emission lines, and a broad deep absorption feature centered near 6900Å, corresponding to the 6909Å, 6946Å CaH bands. Since this feature is not often seen in dCs, and since the C_2 bands appear weak, we believe that this is a spectroscopic composite system that also contains an M dwarf. Together with the as yet unseen white dwarf, this represents the first known dC triple system. For the M star to still have C/O<1, it is likely farther from the former AGB star than the dC, so we speculate that the Balmer emission lines come from interaction between the dC and the white dwarf, which is nevertheless too cool to contribute significantly to this spectrum (and undetected by GALEX).

16. Conclusions

All the data we have gathered and analyzed here remain consistent with the hypothesis that all dCs were "innocent bystanders" to mass accretion in binary systems. The more massive initial primary star evolved up

the AGB, producing a carbon-enhanced stellar wind accreted by its companion main-sequence star, which now bears the atmospheric traces of carbon as a dC star.

Most FHLC stars coincide in color-magnitude space with the locus of "thick-disk-like" ([Fe/H] = −0.7) stars (de Jong et al. 2010). The brighter G-type FHLCs instead coincide with turn-off stars of older, thick-disk or 'inner-halo-like" stars of intermediate metallicity ([Fe/H]= −1.3). We find a high (68%) UV detection rate of G-type FHLC stars, but being similar to the detection rate of generic high proper motion stars of similar color, this is not evidence for hot white dwarf companions.

Thus, they are clearly in systems where the intial primary has already turned off the main sequence, and indeed completed the AGB phase. If the mass ratio q of binary systems peaks near unity (Reggiani & Meyer 2011), then most dCs should be close to the turnoff mass, especially if the mass accretion is enhanced in higher mass bystanders. However, above a certain mass and effective temperature, the formation of C_2 molecules is suppressed, and at some point the C_2 features by which our FHLCs are identified diminish below detectability. Higher mass objects might still be identified e.g., as carbon-enhanced metal poor stars, but only with spectroscopy of significantly higher resolution and S/N.

We may reasonably hypothesize that dCs have or will evolve into Ba or CH giants or subgiants, with a range of properties dependent on their masses and enrichment histories. Further study of the binarity, masses, and/or kinematics of this sample would help to investigate this hypothesis. Post-MTB dwarfs more massive than the G-type FHLC stars currently show no signs of C_2, but while they are therefore not included in our sample, we hypothesize that they must exist, and are best found through spectroscopy of higher resolution, or by far-UV detection of hot white dwarf companions.

Only a handful of the "smoking guns" - systems where the AGB remnant is easily discerned in the optical spectrum or by UV excess - have been found. In the current work, we expand from 2 to 8 the number of such systems known, and we describe them fully in a companion paper (Green 2013).

REFERENCES

Aaronson, M., Liebert, J., & Stocke, J. 1982, ApJ, 254, 507

Aaronson, M., Hodge, P. W., & Olszewski, E. W. 1983, ApJ, 267, 271

Agüeros, M. A., Anderson, S. F., Covey, K. R., et al. 2009, ApJS, 181, 444

Alksnis, A., Balklavs, A., Dzervitis, U., et al. 2001, VizieR Online Data Catalog, 3227, 0

Battinelli, P., & Demers, S. 2006, A&A, 447, 473

Böhm-Vitense, E., Carpenter, K., Robinson, R., Ake, T., & Brown, J. 2000, ApJ, 533, 969

Bothun, G. et al. 1991, AJ, 101, 2220

Covey, K. R., et al. 2007, AJ, 134, 2398

Covey, K. R., Agüeros, M. A., Green, P. J., et al. 2008, ApJS, 178, 339

Dahn, C. C., Liebert, J., Kron, R. G., Spinrad, H., & Hintzen, P. M. 1977, ApJ, 216, 757

Davis, S. P. 1987, PASP, 99, 1105

Dearborn, D. S. P., Liebert, J., Aaronson, M., et al. 1986, ApJ, 300, 314

de Jong, J. T. A., Yanny, B., Rix, H.-W., et al. 2010, ApJ, 714, 663

de Kool, M., & Green, P. J. 1995, ApJ, 449, 236

Demers, S., & Battinelli, P. 2007, A&A, 473, 143

Downes, R. A., Margon, B., Anderson, S. F., et al. 2004, AJ, 127, 2838

Dufour, P., Bergeron, P., & Fontaine, G. 2005, ApJ, 627, 404

Dufour, P., Fontaine, G., Liebert, J., Schmidt, G. D., & Behara, N. 2008, ApJ, 683, 978

Evans, I. N., et al. 2010, ApJS, 189, 37

Gould, A., & Kollmeier, J. A. 2004, VizieR Online Data Catalog, 215, 20103

Gray, R. O., & Corbally, C., J. 2009, Stellar Spectral Classification by Richard O. Gray and Christopher J. Corbally. Princeton University Press, 2009. ISBN: 978-0-691-12511-4

Gray, R. O., McGahee, C. E., Griffin, R. E. M., & Corbally, C. J. 2011, AJ, 141, 160

Green, P. J., Margon, B., & MacConnell, D. J. 1991, ApJ, 380, L31

Green, P. J., & Margon, B. 1994, ApJ, 423, 723

Green, P. J. 2013, ApJ, submitted

Hall, P. B., & Maxwell, A. J. 2008, ApJ, 678, 1292

Harris, H. C., Dahn, C. C., Walker, R. L., et al. 1998, ApJ, 502, 437

Heber, U., Bade, N., Jordan, S., & Voges, W. 1993, A&A, 267, L31

Izzard, R. G., Glebbeek, E., Stancliffe, R. J., & Pols, O. R. 2009, A&A, 508, 1359

Izzard, R. G., Dermine, T., & Church, R. P. 2010, A&A, 523, A10

Joyce, R. R. 1998, AJ, 115, 2059

Karachentsev I.D., Karachentseva V.E., Huchtmeier W.K., & Makarov D.I. 2004, AJ, 127, 2031

Kinemuchi, K., Harris, H. C., Smith, H. A., et al. 2008, AJ, 136, 1921

Koester, D., & Knist, S. 2006, A&A, 454, 951

Kowalski, P. M. 2010, A&A, 519, L8

Kraus, A. L., & Hillenbrand , L. A. 2007, AJ, 134, 2340

Laughlin, G., Bodenheimer, P., & Adams, F. C. 1997, ApJ, 482, 420

Lee, Y. S., Beers, T. C., Sivarani, T., et al. 2008, AJ, 136, 2022

Liebert, J., Schmidt, G. D., Lesser, M., et al. 1994, ApJ, 421, 733

Lloyd Evans, T. 2010, Journal of Astrophysics and Astronomy, 31, 177

Lü, P.K. 1991, AJ, 101, 2229

Lucatello, S., Tsangarides, S., Beers, T. C., Carretta, E., Gratton, R. G., & Ryan, S. G. 2005, ApJ, 625, 825

Margon, B., Anderson, S. F., Harris, H. C., et al. 2002, AJ, 124, 1651

Martin D. C. et al., 2005, ApJ, 619, L1

McClure, R. D., & Woodsworth, A. W. 1990, ApJ, 352, 709

McClure, R. D. 1997, PASP, 109, 536

McConnachie, A. W. 2012, AJ, 144, 4

Mould, J. et al. 1985, PASP, 97, 130

Moultaka, J., Ilovaisky, S. A., Prugniel, P., & Soubiran, C. 2004, PASP, 116, 693

Munn, J. A., Monet, D. G., Levine, S. E., et al. 2004, AJ, 127, 3034

Olszewski, E. W., Aaronson, M., & Hill, J. M. 1995, AJ, 110, 2120

Pagano, I. 2009, Ap&SS, 320, 115

Plez, B., & Cohen, J. G. 2005, A&A, 434, 1117

Reggiani, M. M., & Meyer, M. R. 2011, ApJ, 738, 60

Salim, S. & Gould, A. 2003, ApJ, 582, 1000

Secchi, A. 1869, Astronomische Nachrichten, 73, 129

Smith, M. C., et al. 2007, MNRAS, 379, 755

Stoughton, C., Lupton, R. H., Bernardi, M., et al. 2002, AJ, 123, 485

Strömberg, G. 1939, ApJ, 89, 10

Tonry, J., & Davis, M. 1979, AJ, 84, 1511

van den Bergh, S. 2000, PASP, 112, 529

Vanture, A. D. 1992, AJ, 104, 1997

Voges, W., et al. 2000, VizieR Online Data Catalog, 9029, 0

Vogt, S. S., Mateo, M., Olszewski, E. W., & Keane, M. J. 1995, AJ, 109, 151

Waelkens C., VanWinkel H., Boegaert E., Trams N.R. 1991 A&A, 251, 495

Wallerstein, G., & Knapp, G. R. 1998, ARA&A, 36, 369

Watson, M. G., Schröder, A. C., Fyfe, D., et al. 2009, A&A, 493, 339

Wright, E. L., Eisenhardt, P. R. M., Mainzer, A. K., et al. 2010, AJ, 140, 1868

York, D. G., et al. 2000, AJ, 120, 1579

Zamora, O., Abia, C., Plez, B., Domínguez, I., & Cristallo, S. 2009, A&A, 508, 909

Zucker, D. B., Belokurov, V., Evans, N. W., et al. 2006, ApJ, 643, L103

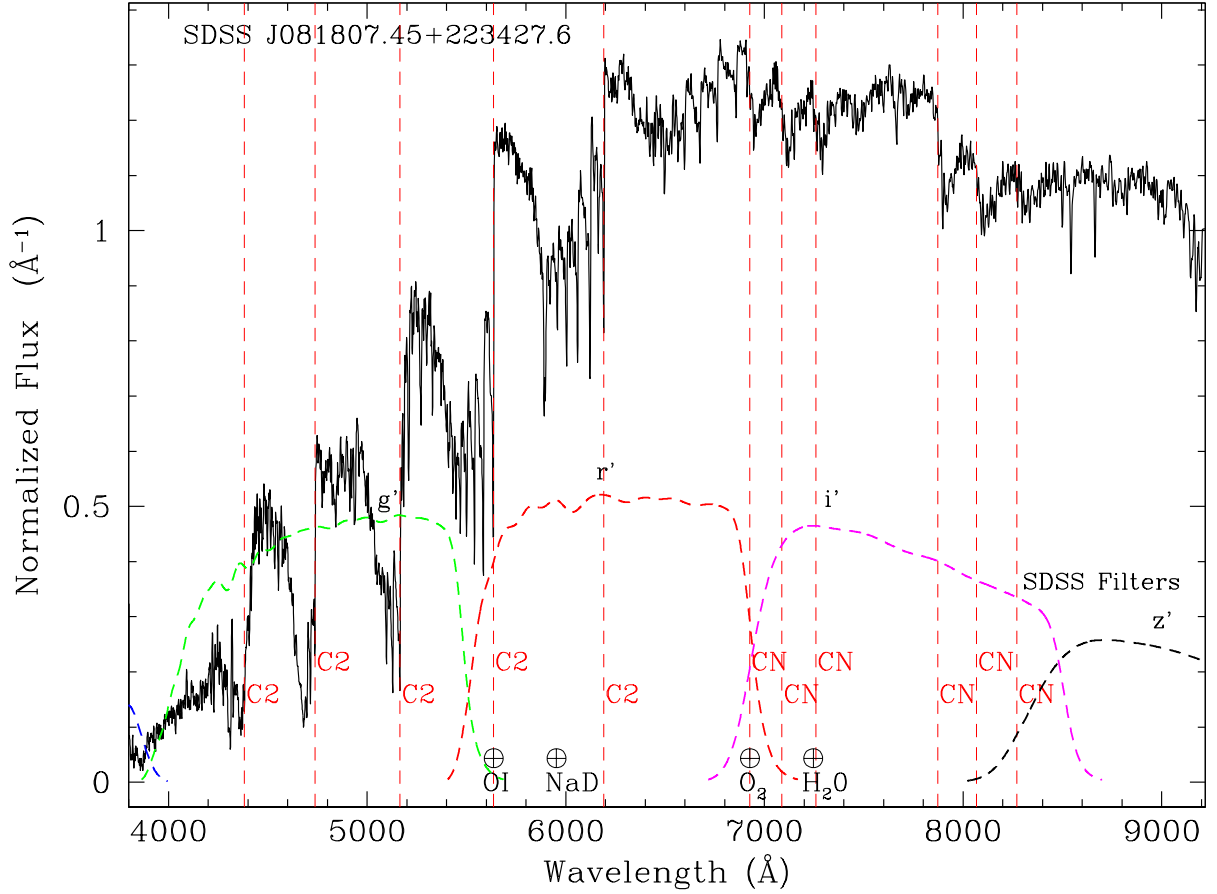Fig. 1.— Spectrum of a typical dC star. This SDSS spectrum of SDSS J081807.45+223427.6, an extreme high proper motion dC star (total proper motion μ=246 mas/year), shows typical C_2 and CN band heads marked with red dashed lines (wavelength list from Davis (1987)). Approximate SDSS *griz* filter transmission curves are shown in dashed lines. Positions of strong potentially telluric features are marked across the bottom.
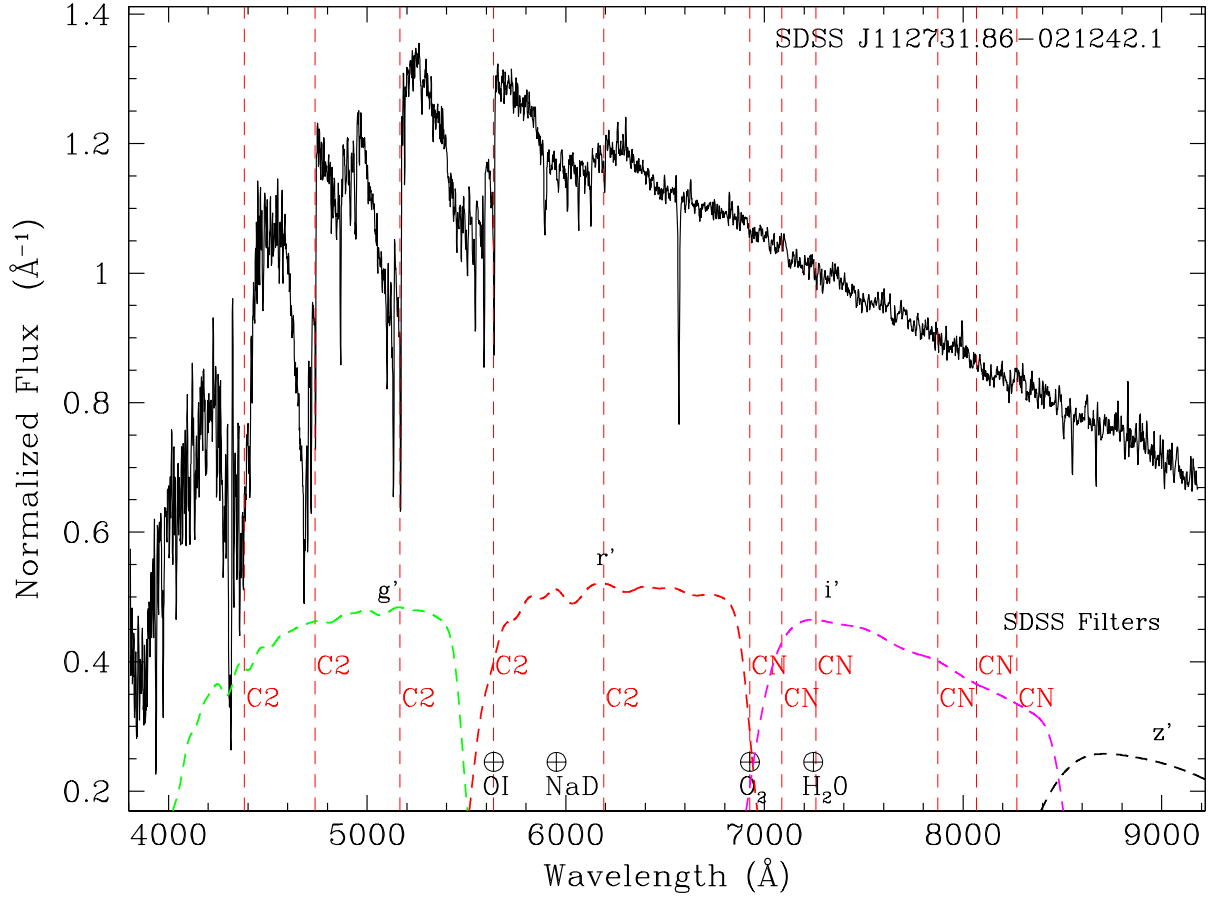
Fig. 2.— Spectrum of a G-type FHLC star. This SDSS spectrum of the G-type dC SDSS J112731.86-021242.1 (μ=42 mas/year) shows features typical of the G-type C stars - blue continuum and no evidence for red CN bands.
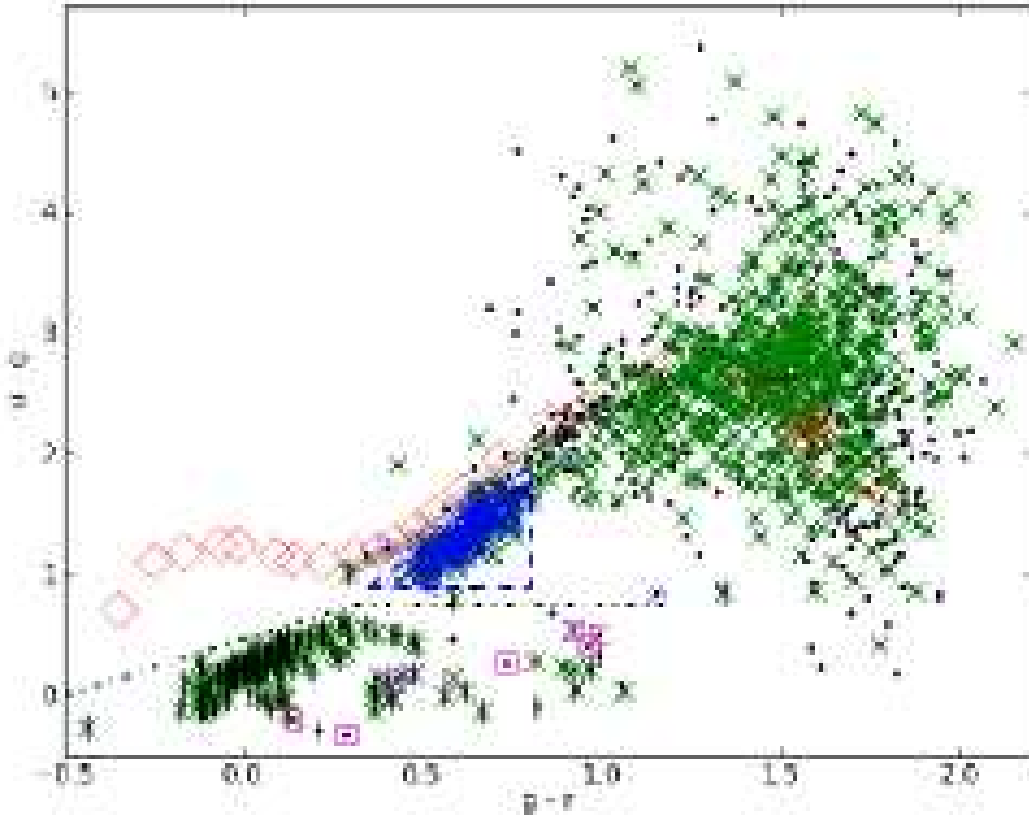
Fig. 3.— Plot of $(u-g)$ vs $(g-r)$ for SDSS stars in our sample (black dots). Objects with significant proper motions (57% of our sample) have their symbols overlaid with a green cross. DQ white dwarfs (vertical bars) and composite DA+dC systems (magenta boxes) are well segregated in this color space by the black dot-dashed line. Blue circles mark the G-type FHLC stars, which are efficiently delineated within the blue dashed triangle. Large red diamonds show colors from the stellar SED compilation of Kraus & Hillenbrand (2007). The median and $\pm 25\%$ grey contours are shown from the SDSS stellar locus of Covey et al. (2007), for types with at least 200 stars in the sample.
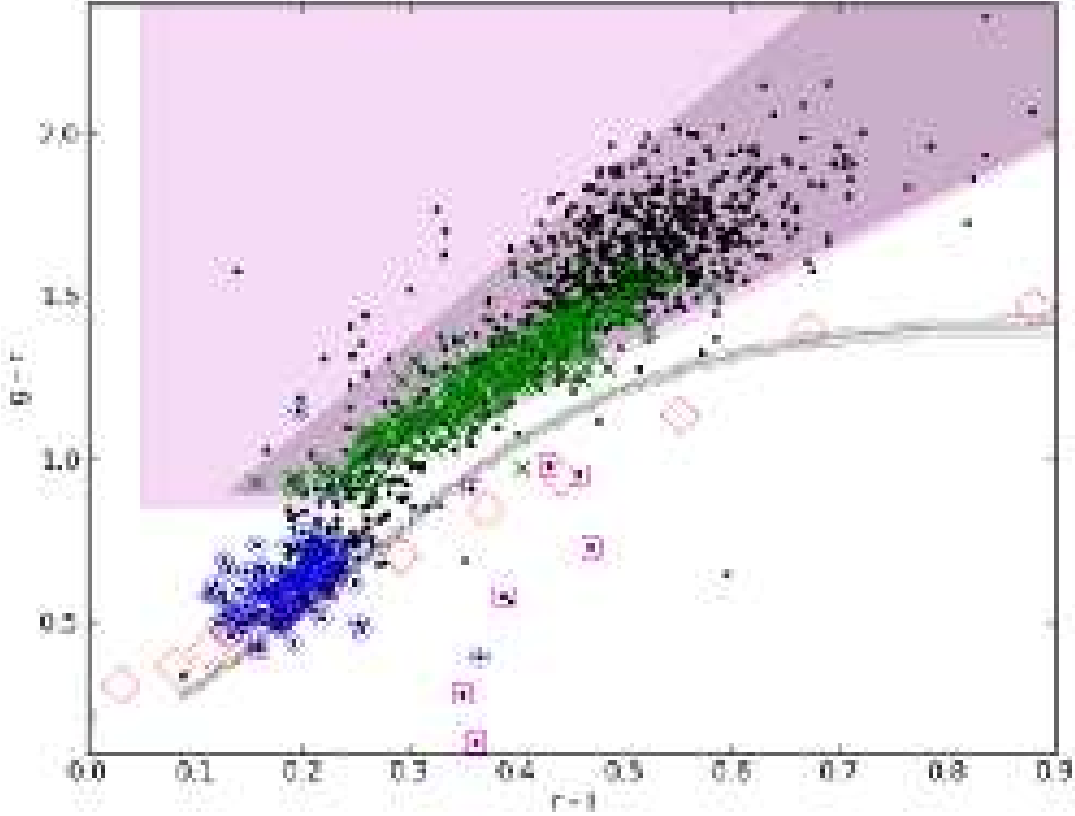
Fig. 4.— Plot of $(g-r)$ vs $(r-i)$ for SDSS stars in our sample (black dots). Symbols are as described in Figure 3, except that here the green crosses show objects targeted by SDSS explicitly as carbon star candidates. Our spectroscopically-selected sample significantly extends the color range of known dCs; only 17% of our sample was targeted as FHLC candidates. DQs have also been removed as in subsequent figures. The light magenta wedge shows the SDSS color selection suggested by Margon et al. (2002). The smaller more deeply-shaded wedge shows the additional criterion used for our FAST dC completeness study described in §15.
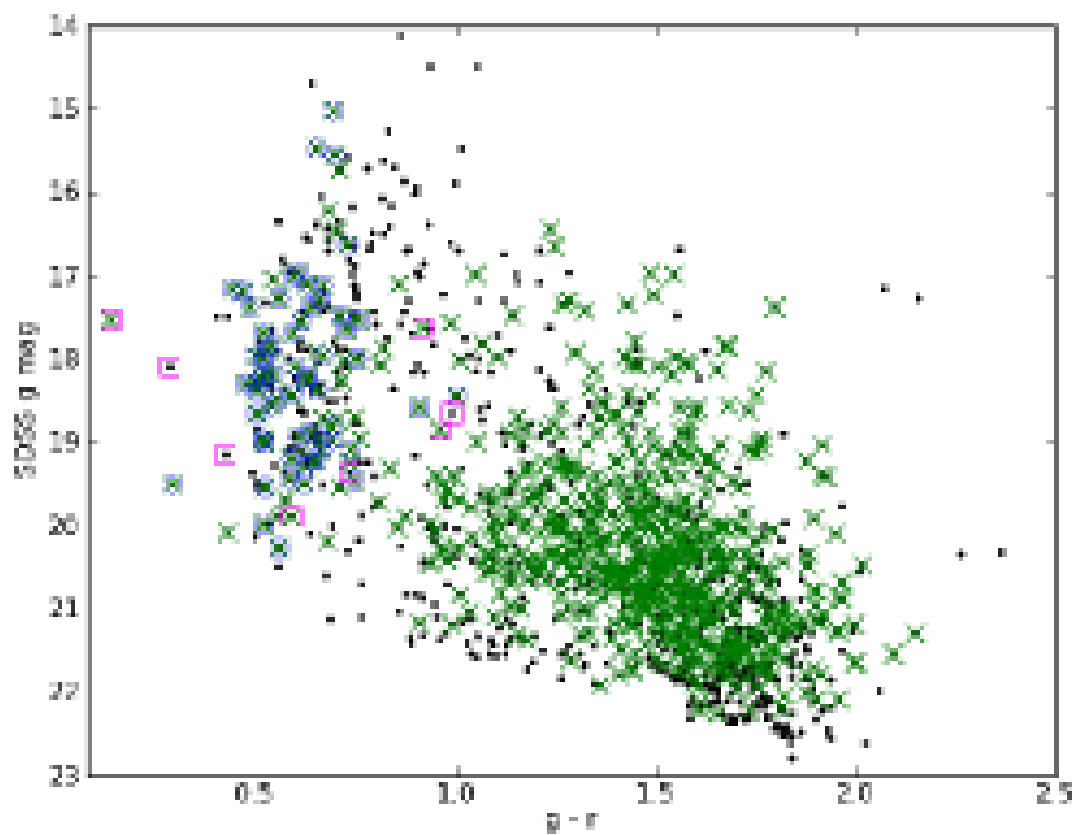
Fig. 5.— Color-magnitude plot of g magnitude vs $(g - r)$ for SDSS C stars in our sample (black dots). Symbols are as described in Figure 3.
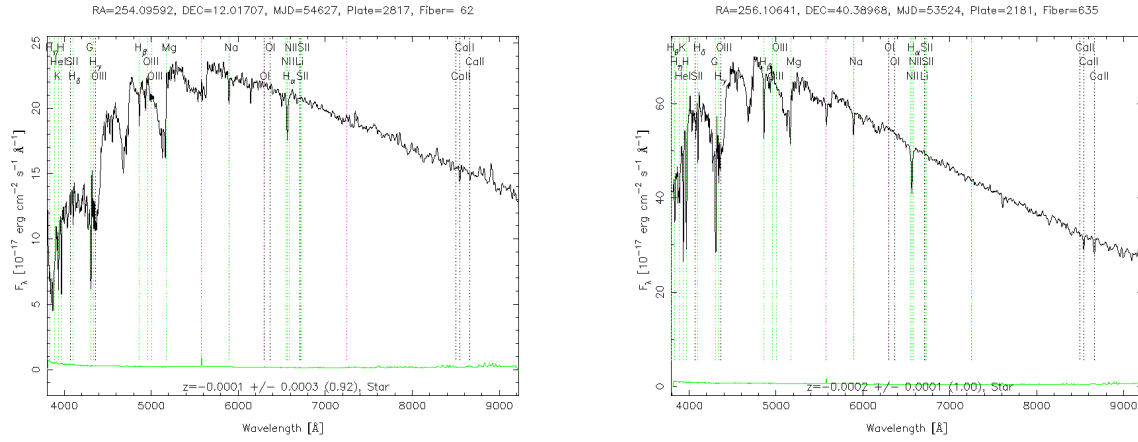
Fig. 6.— Representative SDSS spectra of G-type stars. G-type stars on the red edge of the clump in Figure 4 (e.g., with $(g-r) > 0.7$ and $0.2 < (r-i) < 0.25$), like SDSS J165623.0+120101.4 (left) have significantly stronger carbon molecular bands than do those at the blue edge (e.g., $(g-r) < 0.5$ and $0.1 < (r-i) < 0.15$), like SDSS J170425.5+402322.8 (right). The lack of identified FHLC stars bluer than this edge may simply be due to the disappearance of C_2 bandheads at warmer temperatures.
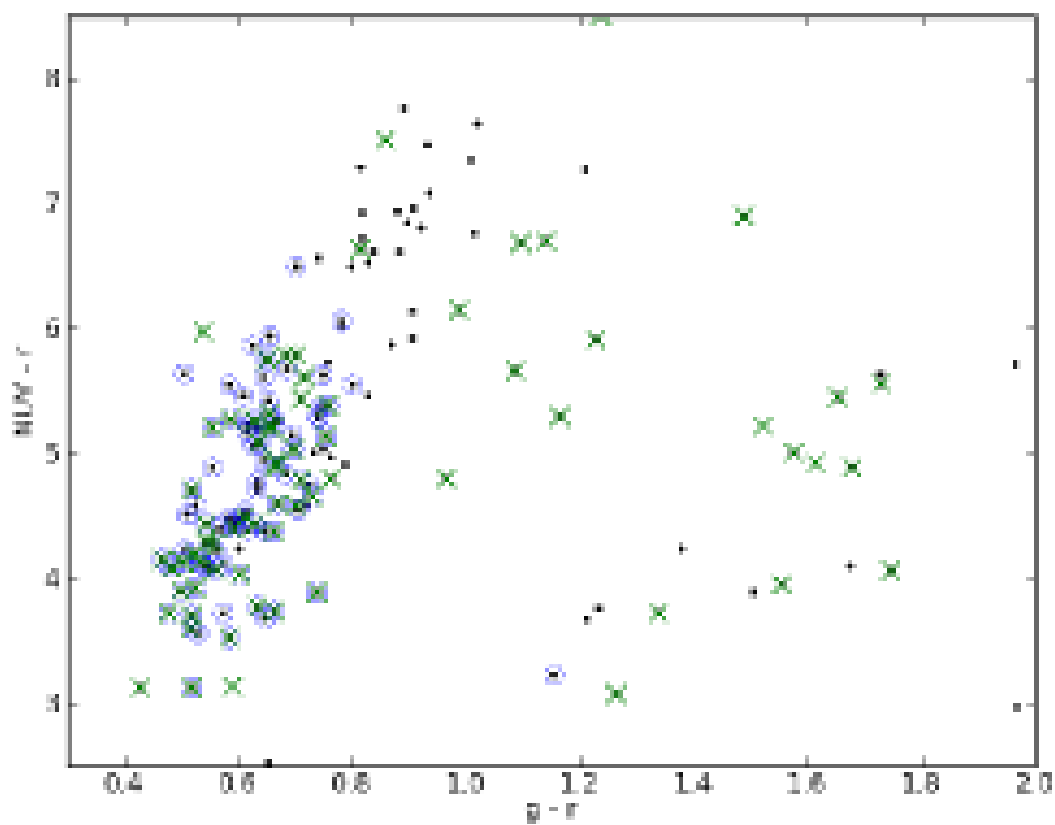
Fig. 7.— Plot of (NUV-*r*) vs (*g* − *r*) colors for SDSS stars in our sample (black dots). G-type FHLC stars are shown as open blue circles. Green crosses indicate objects with significant proper motion.
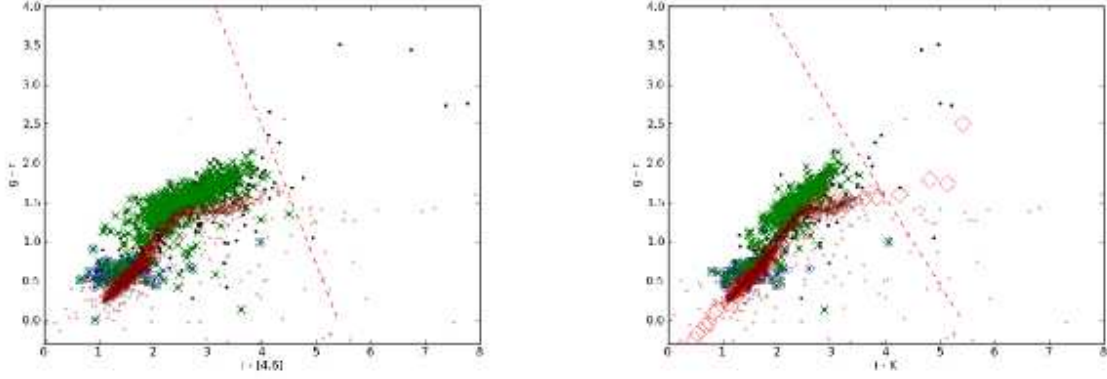
Fig. 8.— LEFT: Plot of (i - [4.6]) vs ($g-r$) colors for SDSS FHLC stars in our sample (black dots) detected by WISE. G-type FHLC stars are shown as open blue circles. Green crosses indicate objects with significant proper motion. Red circles are generic high proper motion dwarfs ($\mu > 20$ mas/yr) from the SDSS DR1/USNO-B catalog of Gould & Kollmeier (2004). The red dashed line at ($g-r$) $> -1.35\,(i-[4.6])+7.5$ shows an effective demarcation for AGB stars. However, either of (i–[4.6])> 4 or ($i-K$)> 3.6 is nearly as clean. RIGHT: Same plot but with (i - K) reveals no clear advantage to use of the WISE mid-IR magnitudes. Large red diamonds show colors from the stellar SED compilation of Kraus & Hillenbrand (2007).
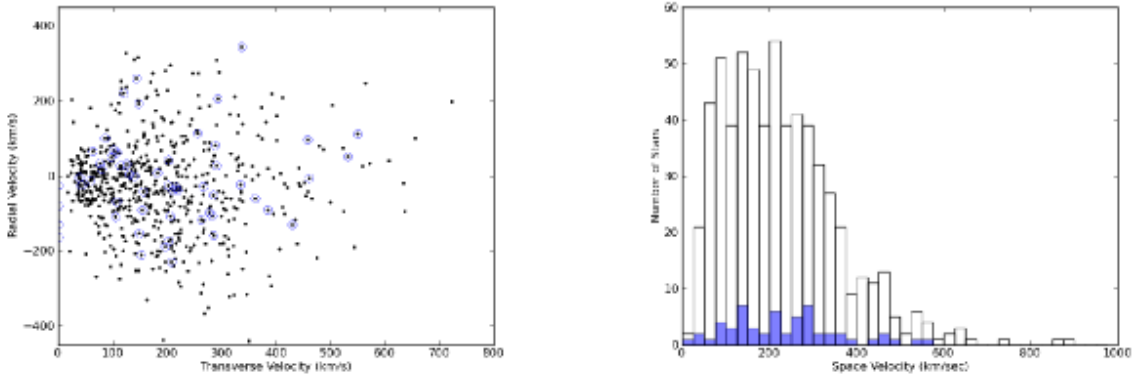
Fig. 9.— LEFT: Plot of the radial velocity derived from comparison to the ELODIE templates vs. estimated transverse velocity for 621 FHLC stars with reliable proper motions (see § 9) and colors suitable for absolute magnitude estimates (see § 10). G-type FHLC stars are shown as blue circles. RIGHT: Histogram of space velocities v_{sp} computed for the same sample. G-type FHLC stars are represented by the shaded blue histogram.
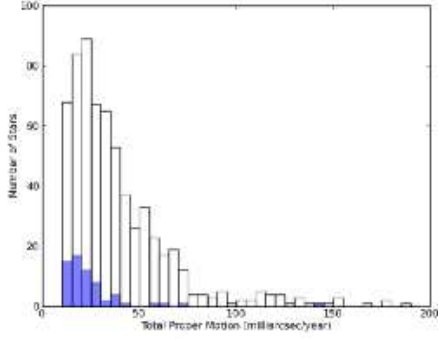
Fig. 10.— Histogram of total proper motion for FHLC stars with significant proper motions, using the criteria in § 9. The blue shaded histogram shows the proper motion distribution for the subset of G-type FHLCs. The lowest bin is not populated because of our criterion that the total proper motion be larger than 11 mas yr^{-1}. 90% of objects with significant proper motion have total proper motion > 15 mas yr^{-1}, which we take as our detection limit.
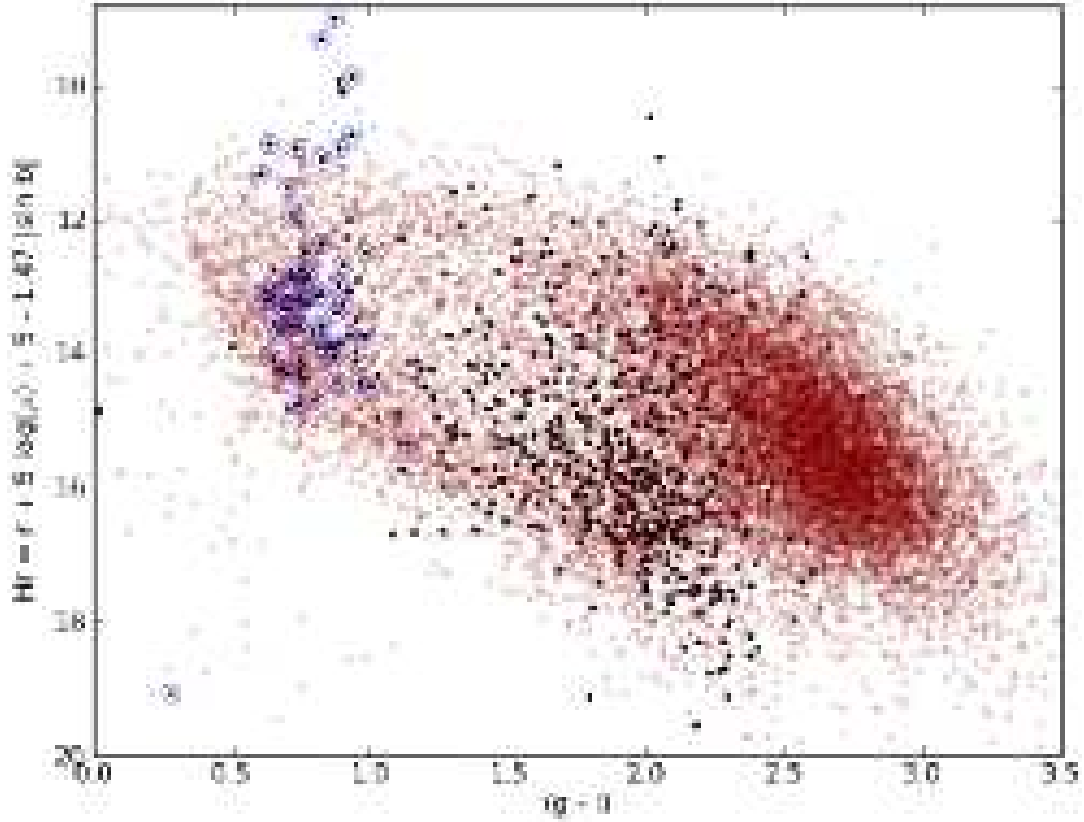
Fig. 11.— Plot of the reduced proper motion vs. $(g-i)$ color for stars with significant proper motions. Small red circles are generic high proper motion dwarfs ($\mu > 50$ mas/yr) from the SDSS DR1/USNO-B catalog of Gould & Kollmeier (2004). G-type stars (blue circles) appear to be blue, and may represent more massive subdwarfs. Other dC stars (black dots), appear to fall between the red dwarfs (densest region on the right), and the subdwarfs (lower diagonal track to the left), indicating they may either be slower moving halo dwarfs, or perhaps thick disk stars.
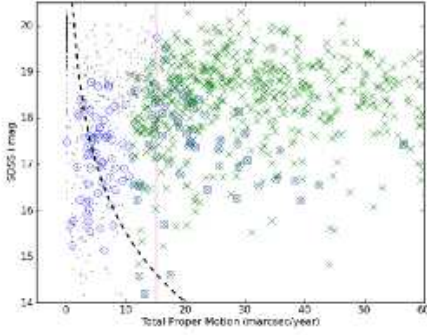
Fig. 12.— Plot of SDSS i magnitude vs. total proper motion in mas/year for FHLC stars. Stars with green crosses have significant proper motions, using the criteria in §9. The vertical magenta line shows our 90% proper motion detection limit of 15 mas/yr. Blue circled points are G-type FHLCs. If we assume that the Galactic escape velocity is 600 km/sec, the green dashed line shows for each proper motion the magnitude fainter than which the star must be a dwarf ($M_i > 3$). Essentially all FHLC stars with detected proper motions in our sample are therefore dCs, with the possible exception of a handful of bright G-type FHLC stars, which may be subgiants.
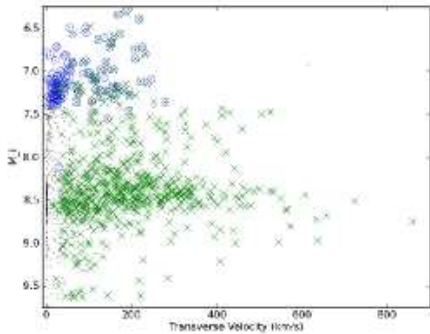
Fig. 13.— Estimated absolute magnitude M_i of FHLC stars vs. transverse velocity v_t, using techniques described in the text. Symbols are as in previous figures. Since no G-type dCs (blue circles) appear to be more luminous than $M_i \sim 6.3$, we adopt this as our criterion to distinguish C giants from dCs.
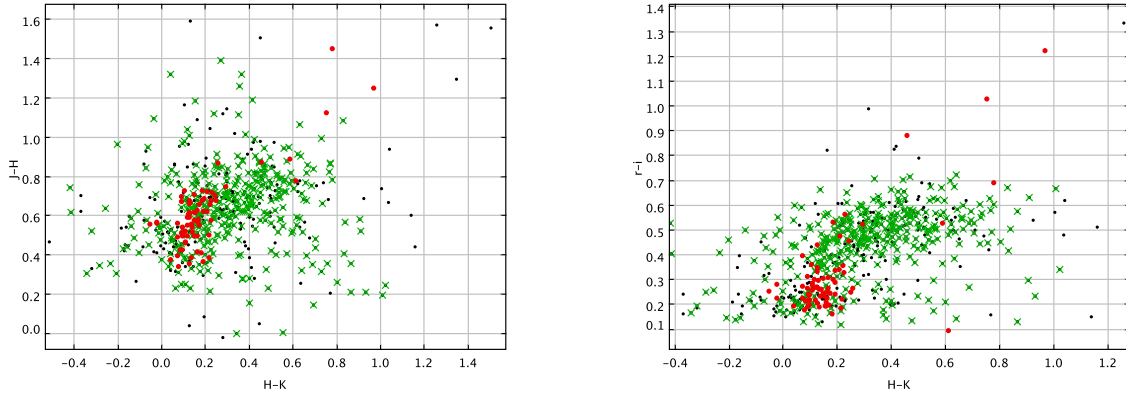
Fig. 14.— Plots of (J-H) vs. (H-K) colors by luminosity class, as determined in § 10. LEFT: Within the magnitude range of our (SDSS spectroscopic) sample of FHLC stars, near-IR colors seem to distinguish a region $(H-K) > 0.3$ where the vast majority of stars are dwarfs (green crosses), with most giants (red dots) clustered at bluer values. RIGHT: Use of $(r-i)$ color for the ordinate axiscreates an even stronger segregation of giants within our sample. However, see Figure 15.
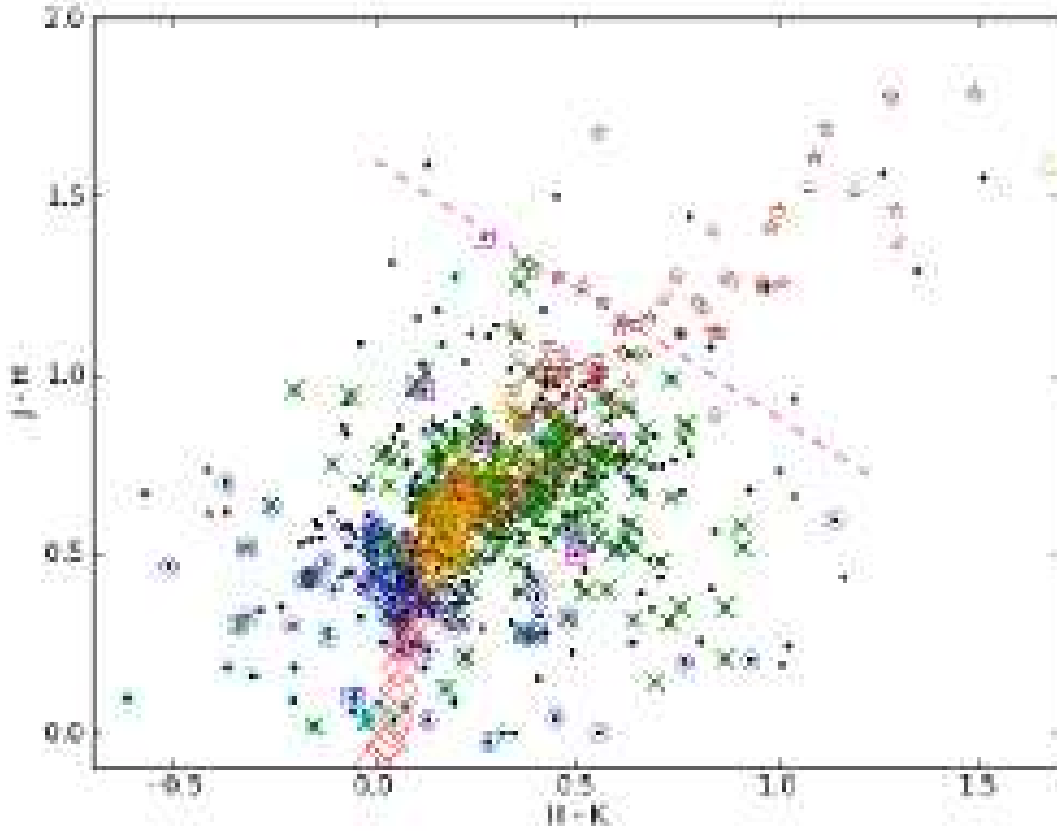
Fig. 15.— Plots of (J-H) vs. (H-K) colors for FHLC stars with UKIDSS or 2MASS detections. Incorporating a wide variety of C stars, we include our SDSS FHLC sample, SDSS DQ white dwarfs (open cyan boxes), as well as N stars (open red stars) and R stars (open orange triangles) from Alksnis et al. (2001). Essentially no star redder than the line $(J-H) = -0.72(H-K) + 1.6$ shows a significant proper motion.
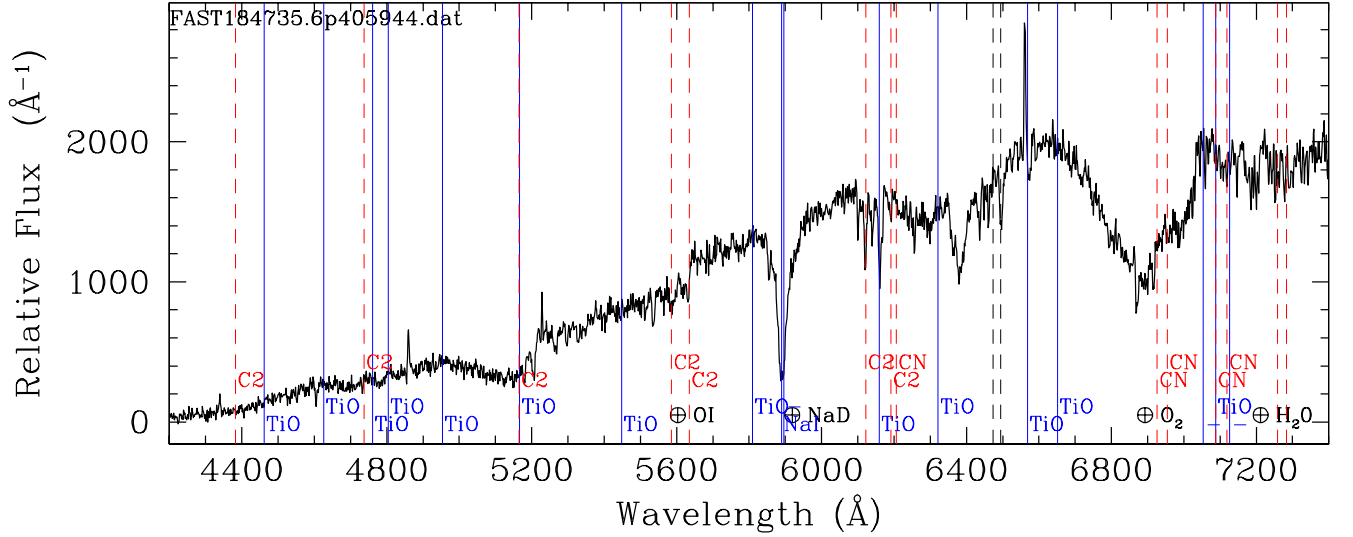
Fig. 16.— FLWO 1.5m/FAST spectrum (flux in ADU) of the most unusual of the 10 dC stars we discovered in our FAST completeness program, SDSS J184735.6+405944. This object shows relatively weak C_2 absorption, strong NaD absorption, strong Balmer emission lines, and broad deep CaH absorption features centered near 6385Å and 6900Å. CaH is only this strong is dwarfs, and was noted in the case of SDSS J153732.2+004343 as a possible luminosity discriminant in low-resolution spectra such as these. The locations of C_2 bands strong in most dCs are marked with vertical red dashed lines; only the 5636Å bandhead is clearly evident. TiO bandheads strong in later M dwarfs are marked with vertical blue lines. None are seen, so we estimate the dC has an M0V companion.

Table 1.   Carbon Stars with SDSS Spectroscopy

Name SDSS J+ [a]	Epoch [b]	r	u-g	g-r	r-i	i-z	J-H [c]	H-K [c]	r-J	NUV	FUV	μ_α	μ_δ	M_i [e]	Cla
												(mas yr^{-1}) [d]			
000015.01+281009.4	52911.21	18.10	1.63	0.81	0.25	0.18	0.72	0.38	1.26	...	...	10.5 ± 3.0	-9.8 ± 3.0	7.24	d
000035.58-001115.0	52231.20	18.80	2.78	1.46	0.48	0.22	0.59	0.24	1.85	...	...	5.7 ± 4.3	-65.4 ± 4.3	8.40	d
000324.63+243815.2	...	17.97	1.28	0.73	0.21	0.17	0.20	0.77	1.58	23.34	...	6.5 ± 2.6	-1.4 ± 2.6	6.80	uG
000354.23-104158.2	51792.43	18.60	4.18	1.39	0.46	0.24	0.69	0.03	1.93	...	...	37.0 ± 3.7	-13.9 ± 3.7	8.33	d
000457.12+010937.9	52231.20	18.39	2.54	1.17	0.39	0.25	0.55	0.03	1.64	...	...	20.7 ± 3.4	-38.9 ± 3.4	8.15	d
000643.14+155800.7	52170.29	19.76	1.92	1.75	0.47	0.14	0.68	0.52	1.93	...	...	-13.0 ± 5.1	-38.3 ± 5.1	8.32	d
000712.54+010757.9	...	18.57	1.76	0.79	0.26	0.12	0.62	-0.37	1.26	24.21	...	3.2 ± 3.4	-2.9 ± 3.4	7.40	u
001145.30-004710.2	...	18.10	2.93	1.52	0.54	0.30	0.68	0.30	1.92	...	...	-4.2 ± 3.0	1.5 ± 3.0	8.50	u
001245.81-010522.0	52910.30	19.55	2.93	1.64	0.48	0.18	0.74	0.49	1.80	...	...	4.6 ± 4.7	-49.9 ± 4.7	8.39	d
001656.41+010549.8	...	17.85	3.05	1.27	0.45	0.44	0.58	0.26	2.17	...	...	0.5 ± 3.2	1.6 ± 3.2	8.33	u
001716.46+143840.8	52170.30	18.34	2.42	1.58	0.51	0.25	0.69	0.30	1.88	...	...	16.2 ± 3.2	-22.8 ± 3.2	8.46	d
001836.23-110138.5	...	18.68	2.21	0.97	0.28	0.20	...	...	...	...	...	8.5 ± 3.8	1.5 ± 3.8	7.49	u
002011.85+002912.2	...	15.76	2.50	1.03	0.27	0.21	0.55	0.13	1.63	23.03	...	-5.5 ± 2.5	-5.9 ± 2.5	7.50	g
002347.62+000528.9	...	16.81	2.52	1.05	0.23	0.24	0.51	0.09	1.64	24.36	...	1.0 ± 2.7	-3.3 ± 2.7	7.23	u
002714.21+002914.3	...	20.74	2.11	1.86	0.54	0.28	1.04	0.22	1.98	...	...	...	...	8.59	nL
002919.44+004314.2	52908.30	18.89	1.34	0.74	0.23	0.12	...	...	...	24.25	...	12.7 ± 3.3	0.2 ± 3.3	7.25	d
003013.10-003226.6	...	19.50	2.01	1.88	0.60	0.16	0.77	0.63	2.10	...	...	7.1 ± 4.7	-7.7 ± 4.7	8.90	u
003351.80+151114.3	...	20.61	1.59	1.74	0.56	0.31	1.50	0.45	1.16	...	...	4.3 ± 5.4	0.8 ± 5.4	8.56	uL
003504.79+010845.9	...	17.85	3.53	1.98	0.80	0.45	0.85	0.50	3.23	23.52	...	-0.5 ± 2.9	3.9 ± 2.9	9.74	uE
003721.34+001224.7	52963.17	19.07	1.95	0.90	0.24	0.18	0.49	0.11	1.51	...	...	19.1 ± 3.3	-19.6 ± 3.3	7.35	d

NOTE: This table is published in its entirety in the online electronic edition of this article. A portion is shown here for guidance regarding its form and content.

[a] Coordinate names are truncated. rather than rounded; precise astrometry is available in the SDSS archive.

[b] Epoch in Modified Julian Day provided for those objects with significant proper motions as described in the text.

[c] Near-IR magnitudes taken from UKIDSS where available, then 2MASS PSC.

[d] Proper motion errors are $\pm 1\sigma$ uncertainties.

[e] M_i calculated from $(r-i)$ color as described in § 10, *assuming* that the object is a main sequence star.

[f] Luminosity Classes (lower case) as described in § 9.1 are d = Dwarf; g = Giant; u = Uncertain; n = No proper motion data. Spectral classes/notes (upper case) a
"G-type carbon star"; E: emission lines; L: low S/N spectrum; N: likely N-type (extremely red, usually strong CN); T: candidate extragalactic object; X: X-ray source;
Draco dwarf galaxy (Draco C-1). A superscript "1" means that the object was already published in (Downes et al. 2004).

Table 2.   Stars in Downes et al. (2004) Not Included in Our Sample

SDSSJ Name
015025.80-001315.1
030837.07+005157.1
032955.54-000354.0
034705.41-063323.9
074710.84+251619.6
080046.72+364107.1
090208.05+435503.8
092545.46+424929.0
100627.47+462117.4
103758.57+612559.3
104138.55+643219.8
105629.95+012208.8
111833.84+563958.1
112836.57+011331.2
113040.49+525039.2
113931.62+050231.2
115925.70-031452.0
121733.35-001857.5
121933.50-012843.0
123834.40+023856.0
143328.12+595808.9
155043.84+571342.5
165141.94+352012.6
231340.54+143600.8

Table 3. DQ White Dwarfs with SDSS Spectroscopy

Name SDSS J+ [a]	Epoch [b]	r	u-g	g-r	r-i	i-z	NUV	FUV	μ_α	μ_δ	Notes
									(mas yr^{-1}) [d]		
000705.02+282104.2	52909.37	19.57	0.34	0.14	-0.06	-0.23	...	...	43.5 ± 4.6	-43.6 ± 4.6	
000807.54-103405.5	51814.36	18.93	0.31	0.07	-0.12	-0.04	20.29	...	0.0 ± 0.0	0.0 ± 0.0	W
002531.50-110800.8	51792.44	18.00	0.22	-0.00	-0.10	-0.17	19.18	...	110.7 ± 3.1	-72.2 ± 3.1	W
010647.93+151327.6	53243.38	19.21	-0.51	-0.35	-0.32	-0.39	...	...	-15.1 ± 3.3	-28.7 ± 3.3	
010748.20+010240.1	52963.19	18.58	0.55	0.24	-0.00	-0.01	20.66	...	20.6 ± 2.9	-169.7 ± 2.9	
015441.74+140307.9	51465.37	17.64	0.56	0.23	0.06	-0.08	20.26	...	165.1 ± 2.8	-220.8 ± 2.8	M
015655.97-005036.3	52224.29	18.89	0.47	0.25	0.03	-0.09	...	...	0.0 ± 0.0	0.0 ± 0.0	
020534.13+215559.7	53269.28	19.50	1.17	0.41	0.06	0.02	...	...	137.8 ± 3.4	36.8 ± 3.4	C
020906.07+142520.7	53710.27	19.16	0.42	0.13	-0.02	-0.03	21.16	...	-23.2 ± 2.9	-48.4 ± 2.9	W
022909.51+251024.4	55119.44	18.84	0.31	0.04	-0.05	-0.12	20.46	...	70.1 ± 2.8	-11.8 ± 2.8	
023609.38-080823.9	54057.23	19.81	0.11	-0.06	-0.10	-0.08	19.86	...	141.6 ± 5.0	42.2 ± 5.0	
023945.01+002745.0	52963.25	19.60	0.45	0.13	-0.03	-0.05	...	...	129.8 ± 3.6	-12.2 ± 3.6	W
024332.74+010112.3	54715.46	20.28	-0.09	0.15	-0.05	-0.33	...	...	59.2 ± 3.4	-121.5 ± 3.4	
024802.27+340802.4	53678.43	18.46	0.72	0.37	0.14	-0.06	21.77	...	-33.7 ± 3.0	-158.7 ± 3.0	
030538.53+055734.3	53655.44	20.67	0.45	0.01	0.02	-0.11	22.63	...	-1.5 ± 5.0	-40.0 ± 5.0	
032054.11-071625.4	51465.45	19.32	0.23	0.43	0.12	0.06	21.09	...	123.6 ± 3.9	-11.7 ± 3.9	P E
033218.22-003722.1	53270.42	18.37	0.21	0.02	-0.06	-0.11	19.62	...	-0.9 ± 5.4	-173.5 ± 5.4	
041601.25+071308.9	54040.43	19.34	0.39	0.21	-0.01	-0.16	21.15	...	11.8 ± 3.3	22.4 ± 3.3	
045032.77-002959.5	53270.47	19.78	-0.01	0.14	-0.01	-0.10	...	...	0.0 ± 0.0	0.0 ± 0.0	
073703.83+645524.6	53293.47	19.52	0.37	0.11	0.00	-0.15	21.20	...	14.1 ± 3.6	-57.7 ± 3.6	

NOTE: This table is published in its entirety in the online electronic edition of this article. A portion is shown here for guidance regarding its form and content.

[a] Coordinate names are truncated. rather than rounded; precise astrometry is available in the SDSS archive.

[b] Epoch in Modified Julian Day provided for those objects with significant proper motions as described in the text.

[d] Proper motion errors are $\pm 1\sigma$ uncertainties.

[f] Notes on spectrum are: C = unusual continuum shape and/or possible composite; E = emission lines; L = low S/N spectrum; M = detected in 2MASS; P = deep molecular bandheads; W = weak molecular bandheads

Table 4.   Dwarf Carbon Stars Confirmed with FAST Spectroscopy

Name SDSS J+ [a]	Epoch [b]	r	u-g	g-r	r-i	i-z	J-H	H-K	r-J	μ_α	μ_δ
										(mas yr^{-1}) [c]	
015856.70+141236.8	51464.37	15.96	2.53	1.25	0.38	0.20	0.53	0.05	1.54	110.6 ± 2.7	-27.5 ± 2
081913.04+023724.0	52318.23	16.16	3.31	1.72	0.00	0.28	0.80	0.38	2.11	-41.6 ± 2.5	-46.2 ± 2
083451.15+074008.7	52667.34	16.56	2.85	1.71	0.00	0.36	0.67	0.32	2.14	49.5 ± 2.8	-39.8 ± 2
093334.14+064812.6	52338.17	15.32	2.67	1.28	0.43	0.25	0.59	0.11	1.74	-9.1 ± 2.5	-43.4 ± 2
093547.66+270938.9	53111.21	15.62	2.49	1.10	0.33	0.16	0.51	0.15	1.58	17.6 ± 2.5	-93.5 ± 2
145725.86+234125.5	53148.34	16.77	2.81	1.79	0.00	0.29	. . .	. . .	. . .	-360.6 ± 2.6	-68.1 ± 2
151040.69+055949.4	52076.21	16.35	2.65	1.27	0.00	0.24	0.60	0.14	1.84	-67.2 ± 12.3	-110.6 ± 12
151702.65+152926.2	53439.48	16.06	2.37	1.03	0.00	0.15	0.57	0.10	1.53	-58.8 ± 2.4	-11.8 ± 2
164035.59+125208.8	53148.41	15.40	2.80	1.36	0.38	0.18	. . .	. . .	. . .	-141.4 ± 2.6	-324.3 ± 2
184735.67+405944.2	53532.40	15.68	2.84	1.95	0.83	0.51	0.70	0.36	2.70	54.5 ± 2.7	-46.7 ± 2

[a] Coordinate names are truncated rather than rounded; precise astrometry is available in the SDSS archive.

[b] Epoch in Modified Julian Day provided for those objects with significant proper motions as described in the text.

[c] Errors are $\pm 1\sigma$ uncertainties

A. SDSS Query for Final FAST dC Candidate Sample

```
-- SDSS DR7 CasJobs query to select carbon dwarf candidates in a color wedge
-- with full criteria used for FAST subsample
-- \protect\vrule width0pt\protect\href{http://casjobs.sdss.org/CasJobs/SubmitJob.aspx}{http://casjobs.sdss.org/C
SELECT p.objID, p.ra,p.dec,
    p.psfMag_r-p.extinction_r + 5*log(sqrt(u.pmRa*u.pmRa + u.pmDec*u.pmDec)/1000.) + 5 AS rpm,
    p.psfMag_g-p.extinction_g-(p.psfMag_r-p.extinction_r) AS gmr,
    p.psfMag_r-p.extinction_r-(p.psfMag_i-p.extinction_i) AS rmi,
    p.psfMag_u, p.psfMag_g, p.psfMag_r, p.psfMag_i, p.psfMag_z,
    p.psfMagErr_u, p.psfMagErr_g, p.psfMagErr_r, p.psfMagErr_i, p.psfMagErr_z,
    p.extinction_u, p.extinction_g, p.extinction_r, p.extinction_i, p.extinction_z,
    p.run,p.rerun,p.camcol,p.field,p.obj, p.status,p.nChild,p.flags,
    u.pmRa, u.pmRaErr, u.pmDec, u.pmDecErr, u.dist20, u.dist22,
    ISNULL(s.specObjID,0) as specObjID, ISNULL(s.specClass,0) as specClass,
    ISNULL(s.z,0) as z, ISNULL(s.zConf,0) as zConf, ISNULL(s.zWarning,0) as zWarning,
    ISNULL(s.plate,0) as plate, ISNULL(s.mjd,0) as mjd,
    ISNULL(s.fiberID,0) as fiberID
  FROM
    PhotoTag p JOIN ProperMotions u ON p.objID = u.objID
    LEFT OUTER JOIN SpecObjAll s ON p.objID = s.bestObjID
  WHERE
    p.dec>-5
    AND p.type = dbo.fPhotoType('Star')
    AND (p.flags & dbo.fPhotoFlags('EDGE')) = 0
    AND (p.psfMag_r-p.extinction_r) BETWEEN 15 AND 17
    AND u.match = 1 AND u.sigRa<350 AND u.sigDec < 350 AND u.nFit > 2
    AND sqrt(u.pmRa*u.pmRa + u.pmDec*u.pmDec) > 40
    AND ( abs(u.pmRa/u.pmRaErr) > 3 OR abs(u.pmDec/u.pmDecErr) > 3 )
    AND ( (p.psfMag_g-p.extinction_g)-(p.psfMag_r-p.extinction_r) )>0.9
    AND ((p.psfMag_r-p.extinction_r)- (p.psfMag_i-p.extinction_i))
        < (0.63*( (p.psfMag_g-p.extinction_g)-(p.psfMag_r-p.extinction_r) ))-0.3362
    AND ((p.psfMag_r-p.extinction_r)- (p.psfMag_i-p.extinction_i))
        > (0.3556*( (p.psfMag_g-p.extinction_g)-(p.psfMag_r-p.extinction_r) ))-0.17
}
```